Lactosylated Polymers for Tissue Engineering

A thesis presented in partial fulfillment of the requirements for the degree of

Master of Science in Chemistry

At Massey University

Shi Zheng

February 2006

Abstract

This thesis describes the synthesis of new polymers suitable for the support of in vitro hepatocyte growth. The key design feature of the monomers investigated was the incorporation of a galactose residue, expected to promote the adhesion and proliferation of hepatocytes in vitro, through the regioselective derivation of lactose.

A graft polymerisation strategy was investigated as an alternative to co-polymerization, since it proved difficult to isolate the carbohydrate-derived monomers in sufficient purity. This led to the formation of a glutaraldehyde-crosslinked lactosylated polyamine hydrogel, which was found to perform well in initial cell trials.

Acknowledgements

Firstly, I would like to thank my supervisors, Roger Lins and David Harding, for the help and guidance I have received over the last two years. I can honestly say that this thesis would not have been completed with the help and support of Roger and David.

I also wish to extend my thanks to others in the group Darren Englebretsen, Veronika Kristova and Libei Guo Bateman. They were wonderful people to work with.

Ms L Green and Associate Professor K Pedley, Institute of Food Nutrition and Human Health (see Appendix: p. 77-81) are thanked for their efforts on the cell studies associated with my research.

Thanks to Pat Edwards and David Lun, for helping me with NMR and MS.

Last but definitely not least, I would like to thank my parents for everything they have done for me and for making me what I am today.

Table of Contents

List of Figures

List of Schemes

List of Tables

List of Abbreviations

ALG	Ca-alginate gels
Azo88	1,1'-azobis (cyclohexanecarbonitrile)
Boc	*tert*-butoxycarbonyl
CD	cyclodextrin
^{13}C DEPT135	carbon distortionless enhancement by polarization transfer
^{13}C NMR	carbon nuclear magnetic resonance
2D COSY	two-dimensional correlation spectroscopy
DCM	dichloromethane
DIEA	*N*-*N*-di-isopropylethylamine
DMF	*N,N*-dimethylformamide
ECMs	extracellular matrices
EDC	1-ethyl-3-(3-dimethylaminopropyl)-carbodiimide
EG	ethylene glycol
ES MS	electron spray mass spectroscopy
FPLC	fast protein liquid chromatography used here for gel filtration chromatography
GC	galactosylated chitosan
HA	hyaluronic acid
HMQC	heteronuclear multiple quantum coherence
^{1}H NMR	proton nuclear magnetic resonance
HPLC	high performance liquid chromatography
IR	infra-red
LCST	lower critical solution temperature
MeOH	methanol
Mw	molecular weight
NVP	*N*-vinyl-2-pyrrolidone
P (.....)	poly (.....)
PAAc	poly (acrylic acid)
PAAm	poly (acrylamide)

PAN	poly (acrylonitrile)
PBO	poly (butylene oxide)
PCL	poly (caprolactone)
PE	propylene fumarate
PEG	poly (ethylene glycol)
PEMA	poly (ethyl methacrylate)
PEO	poly (ethylene oxide)
PGEMA	poly (glucosylethyl methacrylate)
PHB	poly (hydroxy butyrate)
PHEMA	poly (hydroxyethyl methacrylate)
PHPMA	poly (hydroxypropyl methacrylamide)
PLA	poly (lactic acid)
PLGA	poly (lactic-co-glycolic acid)
PMMA	poly (methyl methacrylate)
PNIPAAm	poly (*N*-isopropyl acrylamide)
PNVP	poly (*N*-vinyl pyrrolidone)
PPO	poly (propyleneoxide)
PS	poly (styrene)
PVA	poly (vinyl alcohol)
PVAc	poly (vinyl acetate)
PVLA	poly (N-*p*-vinylbenzyl-4-*o*-β-D-galactopyranosyl-D-gluconamide)
RGD	arginine-glycine-aspartic acid sequence
RT	room temperature
Sty	styrene
TE	tissue engineering
TEMED	*N,N,N',N'*-tetramethyl-ethylenediamine
TFA	trifluoroacetic acid
UPD	under potential deposition
UV-Vis	ultraviolet-visible
VAc	vinyl acetate
Mc	Molecular wight of the crosslinked gel

TBTU	O-(Benzotriazol-1-yl)-*N,N,N′,N′*-tetramethyluronium tetrafluoroborate

Chapter 1: Introduction

1.1 Tissue Engineering

The loss or failure of tissue due to injury or ageing is one of the major causes for concern in human health care. Tissue or organ transplantation is a generally accepted therapy to treat these conditions. However according to the American Liver Foundation report (1988),[1] there were approximately 30,000 patients in the United States who died due to liver failure every year. The availability of donor organs was only around 3,000 per annum. Therefore organ transplantation is extremely limited by donor shortage, and other limitations, such as immunosuppression.

An exciting strategy is to treat patients in need of a new organ or tissue with engineered artificial organs or tissues. Tissues or organs can be potentially engineered through a number of different strategies. In the past few years, three basic strategies have been used. The first method is to use biological factors to stimulate endogenous cells to induce new tissue production. The purpose for the use of biological factors is to initiate cell migration, proliferation and differentiation of the desired cell type from the surrounding tissues.[2] The second method is to encapsulate cells within a semipermeable membrane to augment limited biochemical functions present in a tissue or organ. A classical example of this method was to encapsulate islets of Langerhans to treat Type I diabetes.[3] However a particularly appealing approach utilizes a combination of a patient's own cells with polymer scaffolds to create new tissue and replace all the functions of deficient tissues or organs. In this approach, tissue-specific cells are isolated from a small tissue biopsy taken from the patient, propagated and then harvested in vitro. The cells are subsequently incorporated into three-dimensional polymer scaffolds that act as analogues to the natural extracellular matrices found in tissues. These scaffolds at the appropriate stage of further tissue development are then transplanted to the desired site in the patient's body. The implanted scaffolds provide space for further new tissue formation, and potentially control the structure and function of the engineered tissue (Figure 1.1). A variety of tissues are being engineered using this approach including fabricated artery, bladder, skin, cartilage, bone, ligament, and tendon.[4,5]

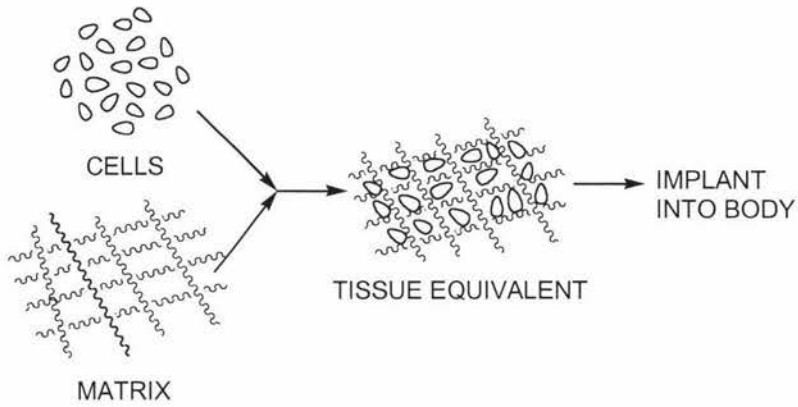

Fig1.1 General strategy for tissue engineering

A critical element in virtually all tissue-engineering approaches is the polymer scaffold. These artificial biomaterials need to replicate the many roles of the extracellular matrix (ECM) in order to support cell survival and growth. They must mimic the functional and mechanical properties of the native ECM. The biomaterials must occupy three-dimensional space in such a way as to bring cells together and control the tissue structure, regulate the growth and function of the cells and allow the diffusion of nutrients, metabolites, and growth factors. Therefore the configuration and structure of these biomaterials are very important for new tissue formation. Studies to date indicate that biomaterials exhibiting high porosity can promote tissue growth through providing a large surface area for cell attachment.[6] Biomaterials produced by tissue engineering (TE) techniques must of course be biocompatible. Some other ideal properties for biomaterials include biodegradablility and robust mechanical and physical properties. Biomaterials should also promote cellular interaction and tissue development.

Cells are cultured in tissue culture flasks coated with media containing growth factors and foetal calf serum. The results over many years in some cases have indicated that cells may lose a number of their characteristics by the process of differentiation.[7,8] For example, isolated chondrocytes (mature cartilage-producing cells) that looked like typical mesenchymal (embryonic cells that form connective tissue) cells that did not build an extra-cellular matrix to a large extent. Therefore the use of novel cell carriers and matrices is needed for reducing (eliminating) cell differentiation. Anchorage of

cells to the substratum is largely responsible for their expression of tissue specific features.[9] Thus, selecting suitable artificial substrata is very important for inducing cell differentiation. Nowadays more and more special proteins, peptides and carbohydrates have been incorporated into artificial substrates to enhance cell adhesion, differentiation and proliferation and to promote new tissue formation.[10]

Tissue engineering is a new and exciting area for research and of course medical advancement in patient care. Many challenges have yet to be met. Examples include maintaining sufficient space within the scaffold framework for prolific tissue development, a space-filling matrix that provides for localization of transplanted cells and a strategy to protect the transplanted cells from lack of essential nutrients.[1]

1.2 Hydrogels and Hydrogels in Tissue Engineering

Hydrogels are polymers crosslinked through covalent chemical bonds and through intermolecular attractions such as ionic interactions, hydrogen bonds and hydrophobic interactions. Hydrogels should possess a three-dimensional structure similar to the macromolecular-based components of the body. These materials absorb water and swell readily without dissolving.[11] Hydrogels have been widely used as biomaterials because of their hydrophilic character and potential for biocompatibility in applications such as wound care products, dental and ophthalmic materials, drug delivery systems, elements of implants, constituents of hybrid-type organs, as well as in stimuli-sensitive systems.[12] Hydrogels have been used as scaffolds on which to engineer new tissues.[13]

Hydrogels are hydrophilic polymer networks that may absorb from 10-20% up to thousands of times their dry weight of water.[14] There are two kinds of hydrogels. The first is named a "reversible" or "physical" hydrogel. The second is called a "permanent" or "chemical" hydrogel. When the networks are held together by molecular entanglements or secondary forces including ionic, H-bonding or hydrophobic forces, they belong to the physical hydrogel class.[15,16] Calcium alginate **(1)** is an example of this kind of gel that is crosslinked through ionic forces. The

interactions in these hydrogels are reversible; therefore by changing physical conditions such as the ionic strength, pH, temperature or by the application of stress these hydrogels can be dissolved or destroyed.[14] When the hydrogels are covalently-crosslinked networks, they belong to the chemical hydrogel class. This kind of hydrogel can be generated by crosslinking water-soluble polymers or by converting hydrophobic polymers to hydrophilic polymers plus crosslinking them to form networks.[14] After crosslinking, hydrogels have an equilibrium swelling level in aqueous solutions. That swelling level depends largely on the crosslink density (estimated by the MW between crosslinks, Mc).[14] The hydrogels may be produced in different physical forms that depend on the end-use. Examples[14] include:

- Solid molded forms for soft contact lenses
- Pressed powder matrices for oral ingestion
- Microparticles for use as bioadhesive carriers or wound treatments
- Coatings on implants, pills or capsules
- Membranes or sheets for use as reservoirs in transdermal drug delivery patchs
- Encapsulated solids for use in osmotic pumps
- Liquids for gel formations on heating or cooling

Many biomaterials have been used to fabricate hydrogels, including natural polymers, synthetic polymers and combinations of natural and synthetic polymers (Table 1.1).[14]

Natural polymers and their derivatives:
Anionic polymers: HA, alginic acid, pectin, carrageenan, chondroitin sulfate, dextran sulfate
Cationic polymers: chitosan, polylysine
Amphipathic polymers: collagen, gelatin, carboxymethyl chitin **(2)**, fibrin
Neutral polymers: dextran, agarose, pullulan
Synthetic polymers:
Polyesters: PEG-PLA-PEG **(3)**, PEG-PLGA-PEG **(4)**, PEG-PCL-PEG **(5)**, PLA-PEG-PLA **(6)**, PHB **(7)**, poly(PF-co-EG) acrylate end groups **(8)**, poly(PEG/PBO terephthalate) **(9)**
Other polymers: PEG-bis-(PLA-acrylate) **(10)**, PEG-g-poly(Aam-co-Vamine) **(11)**, PAAm **(12)**, poly(NIPAAm-co-AAc) **(13)**, poly(NIPAAm-co-EMA) **(14)**, PVAc **(15)**, PVA **(16)**, PNVP **(17)**, poly(MMA-co-HEMA) **(18)**, poly(AN-coallyl sulfonate) **(19)**, poly(biscarboxy-phenoxy-phosphazene) **(20)**, poly(GEMA-sulfate) **(21)**
Combinations of natural and synthetic polymers:
poly(PEG-co-peptides) **(22)**, alginate-g-(PEO-PPO-PEO) **(23)**, poly(PLGA-co-serine) **(24)**, collagen-acrylate **(25)**, alginate-acrylate **(26)**, poly(HPMA-g-peptide) **(27)**, poly(HEMA/Matrigel) **(28)**, HA-g-NIPAAm **(29)**

Table 1.1 Some examples of polymers that are used in the preparation of hydrogels

Hydrogels based on natural or synthetic polymers or a combination of both have found numerous applications in tissue engineering as well as in drug delivery.[17] Tissue engineering is a more recent application of hydrogels, in which they are used as extracellular matrices to repair and regenerate a wide variety of tissues or organs.[14] Hydrogels that are designed for use as tissue-engineering scaffolds should contain pores large enough to accommodate living cells. They may be designed to dissolve or degrade away over a period of time. They may be designed to release growth factors and create pores into which living cells may penetrate and proliferate.[17] There are some advantages associated with the use of hydrogels as matrices in tissue engineering. Firstly, the aqueous environment of hydrogels can protect cells and fragile drugs; secondly, good transport of nutrient to cells and products from cells is

possible; thirdly, hydrogels can be modified with cell adhesion ligands and fourthly, hydrogels can be implanted in vivo. The hydrogel should also be biocompatible at body temperature. Disadvantages existing for hydrogels in tissue engineering include handing difficulties, mechanical weakness and sterilization difficulties.[14,18]

1.3 Design Parameters for Hydrogels in Tissue Engineering

Hydrogels serving as extra-cellular matrices for tissue engineering have many desirable requirements for appropriate function and the promotion of new tissue formation. Physical parameters such as degradation and mechanics, and biological parameters such as biocompatibility and cell adhesion, must be customized to suit the desired application.

Biocompatibility is necessary for the successful culture of cells in the hydrogel. The hydrogels must be non-toxic and should be relatively inert and not interfere with cell functions. Biocompatibility is usually a function of the materials that are used to synthesize the hydrogels. The materials for ECMs should have the ability to be excreted from the body without damaging cells or leaving significant scarring. Polymers derived from natural sources usually demonstrate adequate biocompatibility, however synthetic polymers sometimes show significant negative responses from the body. Therefore some restrictions apply to the choice of synthetic polymers for tissue engineering.[17]

The gelling mechanism is controlled by the type and density of the cross-linking. Three types of gelling are common; ionic, covalent and inherent phase transition behaviour. Ionic cross-linking is a simple way to form hydrogels, however ions can be readily exchanged with other ionic molecules in aqueous environments leading to deterioration of the properties of the original hydrogels.[19] Covalent cross-linking is a good way to elicit precise control over the density of the gel. Covalent cross-linking however can sometimes introduce toxicity or reduce the effectiveness of biodegradation of the hydrogel, and hence produce a negative effect for use in vivo.[17] Use of phase transition behaviour of certain polymers is another way to form hydrogels. This involves changing the temperature near the lower critical solution

temperature (LCST) to initiate the phase transition of a polymer solution to form a hydrogel. The LCST can be designed to be close to body temperature.[20]

The mechanical properties of hydrogels mainly depend on the original rigidity of polymer chains and the type and density of cross-linking.[22] Other mechanical properties relate to the creation and maintenance of a space for tissue development.[21] Degradation is another critical designable parameter in tissue engineering either for natural or synthetic hydrogels. Degradation can be due to hydrolysis or the action of enzymes.[17] Degradation rates and mechanical properties of cross-linked gels are usually coupled to each other, but sometimes those properties can be decoupled by intentionally introducing network defects.[17]

1.4 Hydrogels for Cell Immobilization

The interactions of cells with hydrogels significantly affect their adhesion as well as migration and differentiation.[19] There are three main methods for cell immobilization in hydrogels; adhesion, matrix entrapment and microencapsulation.[23] Each of them has different objectives, therefore selecting the right technique heavily depends on the intended application.

1.4.1 Adhesion

Adhesion of cells to the polymer substrate can either be by surface adhesion to the hydrogel films or by inclusion within hydrogel foams. The adhesion may be cell-type specific and dependent on the interaction of specific cell receptors with ligands displayed on the hydrogel surface.[24] Immobilizing cells by adhesion is likely to stabilize cells for culture or analytical procedures. In addition to the general requirements for TE hydrogels, successful immobilization by adhesion depends on cell attachment to the hydrogel with the preservation of cell function. Many factors affect cell affinity and behavior on hydrogels. These include the chemical composition of the monomers and crosslinkers[25] used as well the hydrophilic/hydrophobic[26] and the surface properties of the hydrogels.[27] Bioadhesive properties can be induced in hydrogels[28], for example by adding cell adhesive peptides, such as the arginine-glycine-aspartic acid (RGD) **(30)** sequence.[29] Physical

properties of hydrogels also affect the cell adhesion; for example, altering pore size and network structure can modify cell adhesion.[30] Collagen in nature is a part of the extracellular matrix. It is usually used in combination with other polymers that are popular as adhesion-based ECMs. This sort of hydrogel can assist in stabilizing cells and provide a growth template, especially for anchorage-dependent cell types.[31]

1.4.2 Matrix entrapment

The difference between adhesion and matrix entrapment is seen in the way the cells are held by the hydrogel. Matrix entrapment depends on physical constraints of the cells within a hydrogel[23] with an open three-dimensional network structure, such that the cells can sit inside properly. The hydrogels should allow efficient transport of nutrients, wastes, and other essential molecules via the bulk fluid. Thus matrix entrapment not only can be used for in vitro applications involving adhesion techniques but can also be used for in vivo studies to protect transplanted cell-hydrogel complexes from mechanical and immunological damage.[23] Matrix entrapment of hepatocytes in collagen was shown to preserve cell functions for much longer than standard culture methods, allowing extended in vitro metabolic studies of liver cells.[32]

1.4.3 Microencapsulation

Microencapsulation surrounds single cells or small clusters of cells with a thin microporous semipermeable membrane. The semipermeable membrane allows the passage of oxygen, important nutrients and cellular products, but it prevents the ingress of immunoglobulins or immune cells responsible for transplant rejection.[33] Diabetes is one of the most heavily investigated clinical example of microencapsulation and the subsequent transplantation of cells.[23] In addition to diabetes, microencapsulation has potential as a treatment for several other diseases and disorders such as Parkinson's disease[34] and liver failure.[35] A selection of existing hydrogels are listed in Table 1.2.

Method	Hydrogel	Cell type
Adhesion	Poly(vinyl alcohol) **(15)**	Corneal epithelial cells
	Poly(2-hydroxyethyl methacrylate) **(31)**	Fibroblasts, Chondrocytes
	Poly(*N*-vinylpyrrolidone-methyl methacrylate-cellulose acetate butyrate) **(32)**	Articular Chondrocytes
	Poly(glycerol methacrylate)/collagen **(33)** Collagen/dermatan sulfate **(34)**	Neuroblasts Vascular endothelial cells
Matrix entrapment	Collagen	Hepatocytes, Esophageal epithelial cells
	Agarose	Erythrocytes, Pancreatic islets
	Alginate	Tumor cells
Microencapsulation	Agarose	Pancreatic islets
	Alginate-polylysine-alginate **(35)**	Pancreatic islets
	Alginate-polylysine-alginate-poly (ethylene glycol) **(36)**	Pancreatic islets
	Poly(2-hydroxyethyl methacrylate-co-methyl methacrylate) **(37)**	PC-12, Pancreatic islets, Hepatocytes, Fibroblasts, Hepatoma cells

Table 1.2 Hydrogels that have been used for cell immobilization[23]

1.5 Problems of Hepatocytes Outside the Organ and Specific Requirements for Hydrogels

With its numerous different indispensable functions, the liver is one of the most important and complex organs in the body. First, it plays a role in glucose metabolism, converting galactose and fructose to glucose and storing glycogen in order to maintain glycemia. Second, the liver is the main organ for lipid metabolism, being the major site of β-oxidation. It is also active in the metabolism of proteins, including urea formation to eliminate ammonia that is toxic for the central nervous system. Moreover, it has a secretory function, synthesizing bile acids for fat digestion and most of the plasma proteins like clotting factors and albumin. Finally, the liver plays a key role in the metabolism of endogenous and exogenous substances in order to facilitate their excretion. These functions are carried out by the hepatocytes, epithelial cells that represent 80% of the liver volume.[36] Therefore maintaining a healthy liver is very important for humans. However, currently, many patients are suffering from loss of liver function. Nowadays liver transplantation is the most effective treatment. Donor shortage and the associated costly surgical procedure are factors limiting its widespread use for patients who suffer from liver diseases. Therefore tissue engineering is a good target for fighting liver failure.

Normally in tissue engineering, the liver cells would be specifically isolated from the patients, and harvested into the particular extra-cellular matrix. However, there is an extremely significant problem for liver cells outside the organ and that is the hepatocytes will lose their cellular functions rapidly and have only limited viability.[37] If cultured hepatocytes could survive and proliferate over long periods of time, such a culture system would permit extensive studies of the basic cellular phenomena and clinical investigations of liver diseases. The system could also serve to produce an artificial organ to make up for the loss of liver function. The polymer scaffold should have abilities to prolong cellular function and viability of hepatocytes outside the body. Moreover hepatocytes are a type of anchorage-dependant cells that are known to rapidly lose their hepatic phenotype in vitro.[38] Hepatocyte anchorage is a strict requirement for the survival of hepatocytes.[39] In order to culture these kinds of cells, scaffolds require specific interaction with extra-cellular matrix components, growth

factors and the cell surface receptors for survival. Therefore, the design and selection of polymer materials are crucial for this application of tissue engineering. Rat hepatocytes have been used in a study by Paul et al.[40] Their results showed that rat hepatocytes adhered specifically to polyacrylamide gels containing galactose residues (Figure 1.2).[40]

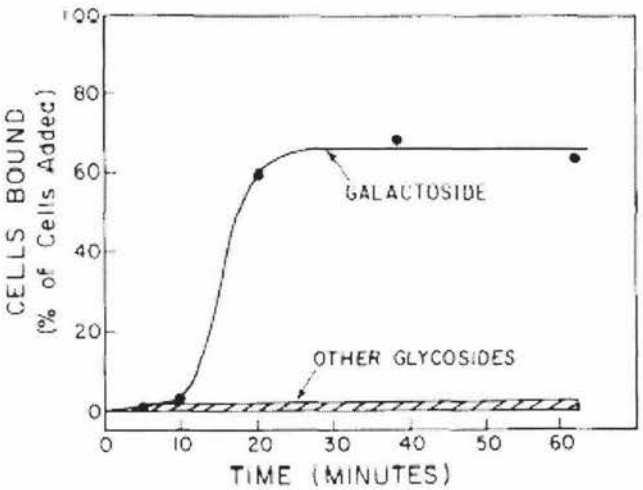

Figure 1.2 Kinetics and sugar specificity of rat hepatocyte binding to polyacrylamide gels[40]

Therefore it is of interest to incorporate galactose residues into polymer scaffolds to promote the cell adhesion. Recently many efforts have been made to develop biological substitutes based on liver cell and polymer matrices.[41] Various polymers derived from natural and synthetic materials that contain galactose residues have been used for extracellular matrices designed for growing liver cells outside the human body. Many natural polymers have been used for extracellular matrix assembly, such as collagen, laminin and fibronectin because they have several globular domains that are specialized for binding to the cells.[42,43] Many new materials have been synthesized to serve as ECMs to replace many of the functions of the natural ECM. Galactose-carrying polystyrene (PS) **(38)** and poly(*N*-p-vinylbenzyl-4-o-β-D-galactopyranosyl-D-gluconamide) (PVLA) **(39)** were reported as artificial ECMs that regulated the proliferation, differentiation, and morphology of hepatocytes.[44-46] Chitosan is another popular material for synthetic ECMs.[47] It is biodegradable, non-toxic[48] and has amino and hydroxyl groups which can be modified chemically. Galactose-containing carbohydrates could be covalently coupled with chitosan for the development of synthetic ECMs for adhesion of the hepatocytes. The result of hepatocyte adhesion to

a galactosylated chitosan (GC) **(40)**-coated polystyrene (PS) dish was 94.7% adhesion after 2h incubation whereas for a chitosan-coated PS control dish, the figure was only 69.1%, indicating galatose is important as a recognition signal for hepatocytes.[47]

Alginate is a naturally derived polysaccharide from seaweed and is a particularly attractive biopolymer that has been extensively used for synthetic ECMs.[49] It is biocompatible, hydrophilic and biodegradable under normal physiological conditions. However if alginate alone is used as an ECM, a mechanically unstable matrix is produced due to the exchange of crosslinked divalent cations with monovalent cations.[50] Unfortunately alginates lack the specific cell-recognition signals that promote the interaction of the anchorage-dependent cells with the matrix. Ca-alginate (ALG) **(1)** gels reacted with galactosylated chitosan (GC) **(40)**, through the electrostatic interaction of carboxylic groups of alginate with the amine groups of GC **(40)**, to form highly porous, three-dimensional sponges. These sponges provided good hepatocyte anchorage sites and enhanced mechanical properties. High viability of the hepatocytes was observed for the ALG **(1)**/GC **(40)** sponge. Only a few cells formed spheroids within the ALG **(1)** sponge, proving that introduction of the galactose moiety into the sponge provided hepatocyte-recognition signals for hepatocyte attachment.[49]

1.6 Choice of Lactose to Build a Sugar-based Polymer Scaffold

In the study reported in this thesis, lactose was chosen to build the sugar-based polymer scaffold. Firstly lactose is a disaccharide that contains a galactose residue and a glucose residue (Figure 1.3). Therefore we can react the glucose residue e.g. via oxidation and acryloylation, and preserve the conformation of the galactose residue for liver cell recognition. Secondly lactose is a readily available commercial product produced in New Zealand.

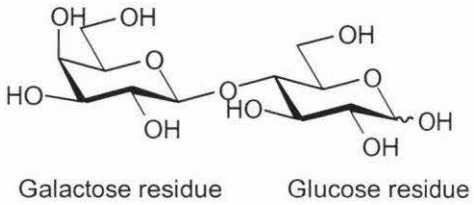

Figure 1.3 The structure of lactose

1.7 Hydrogels from Synthetic Polymers – Copolymer of Lactose and N-isopropylacrylamide

Lactose has a bulky three dimensional molecular structure; therefore, we need to use another small active compound to co-polymerize with the bulkier lactose derivatives. This will help to reduce crowding from too many lactose residues which could possibly lead to inactivity. We chose *N*-isopropylacrylamide as our copolymer component in the hydrogel. Poly(*N*-isopropylacrylamide) PNIPAAm **(41)** is potentially very attractive for tissue engineering applications as it exhibits phase transition behaviour above its lower critical solution temperature (LCST).[19] The LCST of PNIPAAm **(41)** in water is approximately 32°C and can be modified to match body temperature by co-polymerization.[51] When the temperature of PNIPAAm **(41)** is above its LCST, the aqueous PNIPAAm **(41)** solutions will turn cloudy because hydrophobic groups in the polymer chain form insoluble aggregates.[52] However the PNIPAAm **(41)** will dissolve again in water as the temperature goes below its LCST. Adding different amounts of hydrophilic or hydrophobic monomers can change the phase behaviour of PNIPAAm **(41)**. The copolymerization of NIPAAm with more hydrophobic monomers decreases the LCST of PNIPAAm **(41)** copolymers, while more hydrophilic monomers tend to have the opposite effect on LCST.[53-57]

PNIPAAm **(41)** was used as model polymer for examining the use of lower critical phase separation systems in tissue engineering applications. Stile and his co-workers[58] used the phase behavior of PNIPAAm-based hydrogels in the development of injectable polymer scaffolds that support tissue formation. Loosely cross-linked PNIPAAm **(41)** and PNIPAAm-co-acrylic acid [PNIPAAm-co-AAc] **(13)** hydrogels

were synthesized for injectable hydrogels. The results showed both hydrogels were pliable and fluid-like at room temperature, but demonstrated a phase transition as the matrix warmed from room temperature to body temperature, yielding more rigid structures.[58] Therefore these hydrogels were good for in situ stabilization.

Most recently, PNIPAAm **(41)** was used to graft onto gelatin to form hydrogels to work as a thermoresponsive artificial extracellular matrix.[59-62] Bovine smooth muscle cells present proliferate well in PNIPAAm-gelatin **(42)** hydrogels with a high weight ratio of PNIPAAm **(41)** to gelatin.[61] More studies were carried out to investigate how the viability and proliferation of cells entrapped in a three-dimensional hydrogel depended on the graft architecture, including graft chain density and graft chain length of the PNIPAAm-gelatin **(42)**.[62]

Therefore, the use of PNIPAAm **(41)** and its copolymers in tissue engineering would be very beneficial as they can easily be prepared in a mixed solution of cells and the polymer at or below room temperature then injected into the desired site. This will result in the formation of a solid cell polymer construct as the gel warms to body temperature. NIPAAm has been copolymerized with acrylic acid, methacrylic acid, or butylmethacrylic acid, depending on the desired final applications.[58,63,64]

1.8 Objectives for this Study

In order to understand more about cell adherence factors, cell behavior outside the human body and to extend the viability of hepatocytes *in vitro*, we have incorporated many of the theories discussed above to synthesize lactose-based copolymers. Figure 1.3 shows the ideal result of hepatocytes bound within the polymer scaffold.[37]

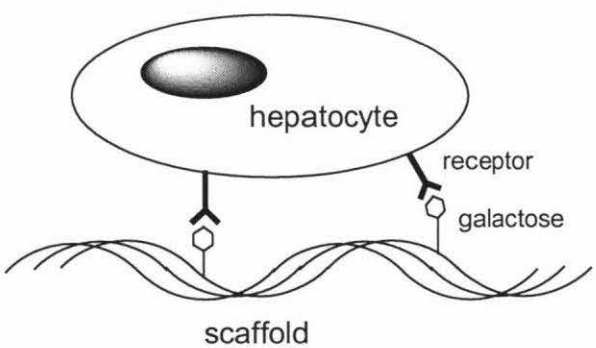

Figure 1.4 Ideal scaffold for binding hepatocytes[37]

The aim of this study is the synthesis of a polymer scaffold of this type to serve as an ECM mimic for growing hepatocytes. The scaffold must contain galactose residues that can help to promote the adhesion, proliferation and viability of hepatocytes *in vitro*. Figure 1.5 illustrates this concept.

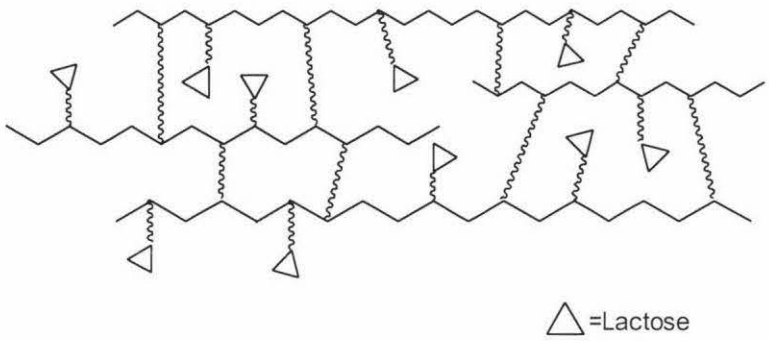

Figure 1.5 Objective hydrogel for ECM

Chapter 2: Preparation of monomers and synthetic polymers

2.1 Oxidation of lactose

According to the project plan, the monomer should contain galactose linked to an active double bond through the glucose residue. The key point of having lactose in the monomer is that liver cells have a special recognition for galactose that will enhance the adherence of hepatocytes to the polymer surface. If the linkage between lactose and the active double bond is part of the glucose residue, the geometry of the galactose residue is maintained throughout the monomer synthesis and the polymerization processes. The resulting polymer should then bind hepatocytes (Scheme 2.1).

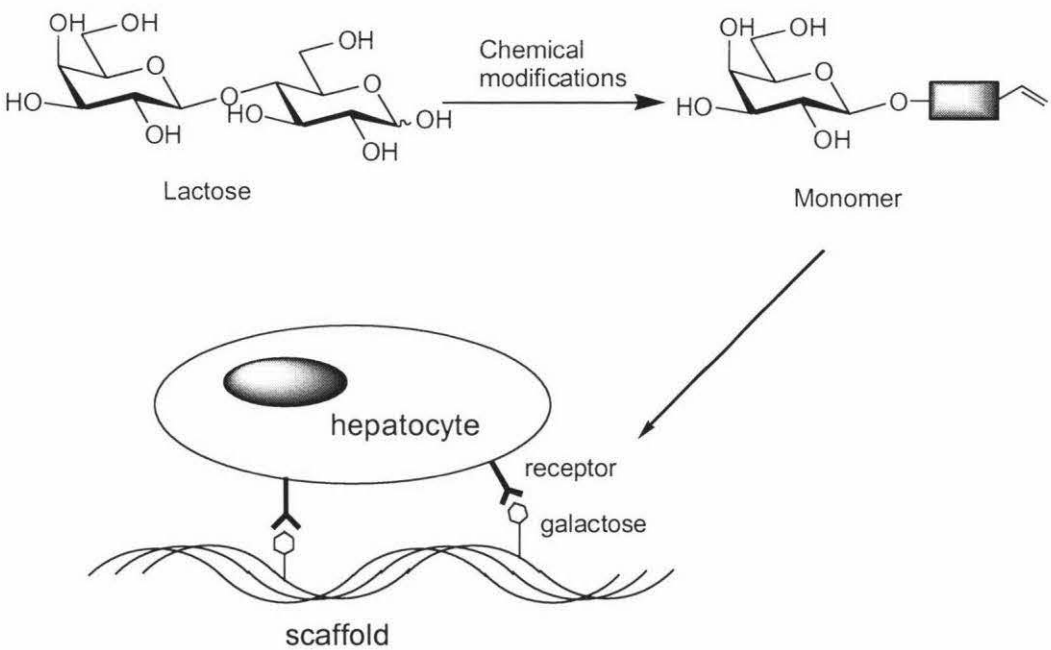

Scheme 2.1. General plan for making lactosylated polymer

Lactose is a reducing sugar; the reducing terminus (glucose) is a hemiacetal in equilibrium with small amounts of the aldehyde (open-chain) form. This is the logical position at which to perform chemical modifications on lactose to meet the objectives of this project. There are three ways to connect through the anomeric centre: firstly

using the hemiacetal directly to make a glycosidic bond; secondly doing a reductive amination to produce an amine; or thirdly doing an oxidation to form an ester or amide bond through the resultant carboxyl group. Due to the biological end uses envisaged for this polymer, the introduction of many charged or basic groups is not appropriate; rather a chemically robust, highly hydrophilic but neutral polymer is desired, and so it was decided to use amide bonds to link lactose and the polymerisable double bond. The synthesis therefore began with oxidation of the reducing terminus (glucose residue) of lactose, with the resulting acid group to be reacted with an appropriate amine bearing an active double bond (Scheme 2.2).

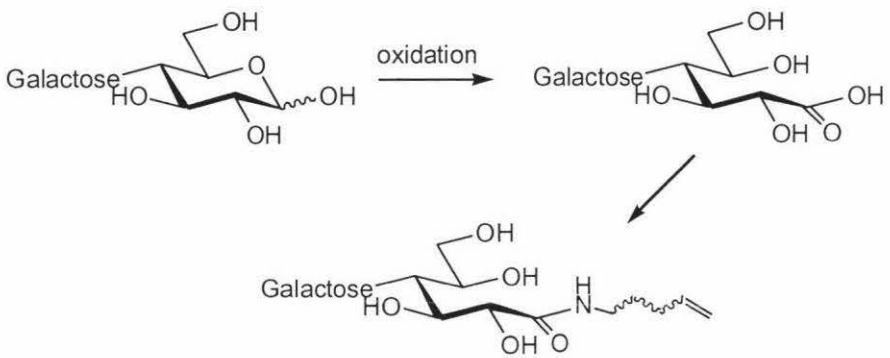

Scheme 2.2. Procedure for amide bond formation

Oxidation is a characteristic reaction of the anomeric centre of reducing sugars, and many methods are available to achieve this. The best known ways are by reaction with a solution of silver ion in aqueous ammonia (Tollens' solution), or with cupric ion (Benedict's or Fehling's reagent), however these are traditional analytical, rather than synthetic methods. Many synthetic methods have been reported to oxidize sugar hemiacetals. For example: Aoun et al. studied the electrocatalytic oxidation of sugars on silver-UPD single crystal gold electrodes in alkaline solutions. The sugars that they studied for this method included aldose-type monosaccharides (glucose, mannose and xylose) as well as reducing disaccharides (maltose and lactose). In their research one significant oxidation peak was obtained, however, no significant oxidation current was observed for disaccharides.[65] Singh et al. used metals as catalysts to oxidize sugar hemiacetals.[66] Firstly they used Ru(III) and Hg(II) as co-catalysts in the oxidation of D-galactose and D-ribose by *N*-bromoacetamide in perchloric acid. The balanced equation is given below:

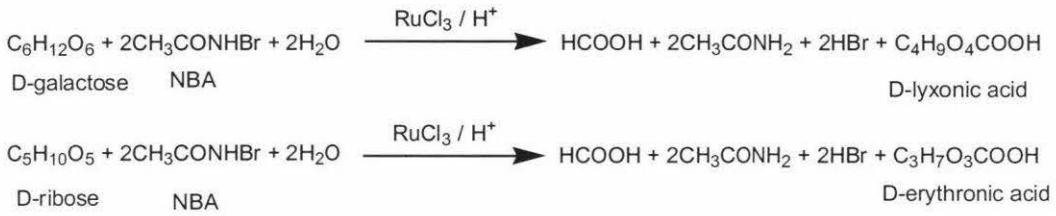

Scheme 2.3. Oxidation equations of D-galactose and D-ribose

Later they used Pd(II) and Hg(II) as co-catalysts in the oxidation of D-mannose and maltose in acidic solutions of *N*-bromoacetamide.(reference). The balanced equation is given below:

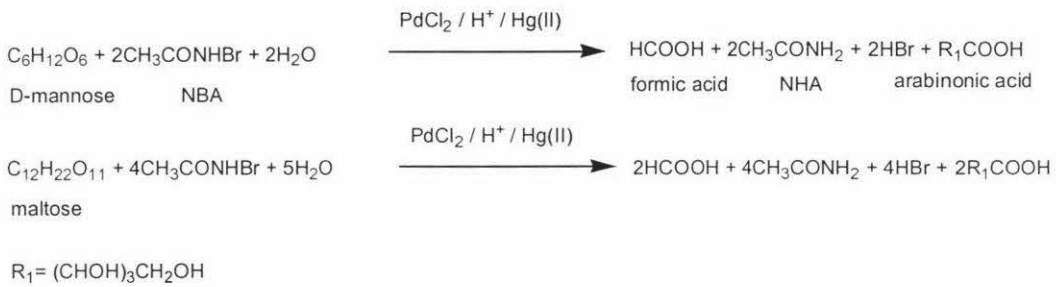

Scheme 2.4. Oxidation equations of D-mannose and maltose

The reaction rates in these oxidations were affected by many factors, and many by-products were produced during the reactions, making this route unsatisfactory for the current purposes. The potassium hypoiodite-methanol procedure has been developed as a simplification of existing methods by the elimination of several operations inherent in other techniques for carrying out the oxidation.[67] The preparation of the potassium salt of gluconic acid in a single operation has been realized by introducing methanol as the reaction solvent for the hypoiodite oxidation. The balanced equation is given below:

Scheme 2.5. Oxidation equation of potassium hypoiodite-methanol procedure

Glucose, iodine, potassium hydroxide, and potassium iodide are all soluble in aqueous methanol. As the reaction proceeds, sparingly soluble potassium gluconate **(43)** precipitates and can be easily recovered by filtration. The general method has been adapted to the oxidation of other reducing sugars.[68]

In the current study, lactose (which has relatively low solubility in water) was first completely dissolved in warm water, before a dark brown solution of iodine in methanol was added. Dropwise addition of a solution of potassium hydroxide in methanol was accompanied by the slow disappearance of the iodine colour, and (provided efficient stirring was maintained) by the deposition of a white crystalline product. The precipitate was filtered and washed with cold methanol and ether to remove the unreacted iodine and lactose, and recrystallised from a mixture of water and methanol. Crystalline potassium lactobionate **(44)** was obtained in high yield (79%) and exhibited the expected spectral properties. Thus, the ^{1}H NMR spectrum of the product exhibited a doublet (J=7.8Hz) at 4.54ppm, assigned to 1'-H_{ax} and indicating retention of the galactose residue in its cyclic acetal (β-galactoside) form. On the other hand, no signals attributable to 1-H were observed, and the signal assigned to 2-H (4.16ppm) appeared as a small doublet (J=3Hz), indicating that the glucose ring was present in an open and oxidized form. The COSY spectrum showed strong clear correlations from 2-H around to 6-H, but none of these signals displayed the large coupling constants characteristic of the *trans*-diaxial relationships between protons in a glucopyranose ring. The correlations from 1'-H to 6'-H were also clear, but in this case the expected *trans*-diaxial relationships were apparent; thus 2'-H (3.57ppm) exhibited reciprocal couplings to 1'-H (J=7.8Hz) and to 3'-H (J=10Hz). 3'-H (3.66ppm) also showed coupling to 4'-H (3.45Hz), the smaller coupling constant being consistent with the equatorial position of the 4'-H proton.

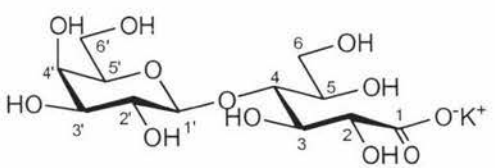

(44)

Further evidence for a successful oxidation was provided by the ^{13}C spectrum, which showed one signal in the carbonyl region (178.5ppm) and one signal in the anomeric region (103.5ppm), assigned to C-1 and C-1' respectively. Finally, the IR spectrum of the product exhibited a strong absorption at 1604cm^{-1}, assigned to carboxyl stretching, and the correct parent ion (M-1=357) was observed in the ES(-) mass spectrum.

Potassium lactobionate **(44)** was thus conveniently prepared, and isolated in a highly crystalline form, but direct reaction of this product with an amino group in aqueous solution is likely to result initially in the formation of ammonium salts, and because of the low reactivity of the carboxylate ion toward nucleophilic substitution, further reaction is unlikely to follow. However water-soluble carbodiimides such as EDC have been used to promote amide formation in mildly acidic aqueous solution, by reacting with the carboxylic acid and activating it toward nucleophilic substitution, as shown below.

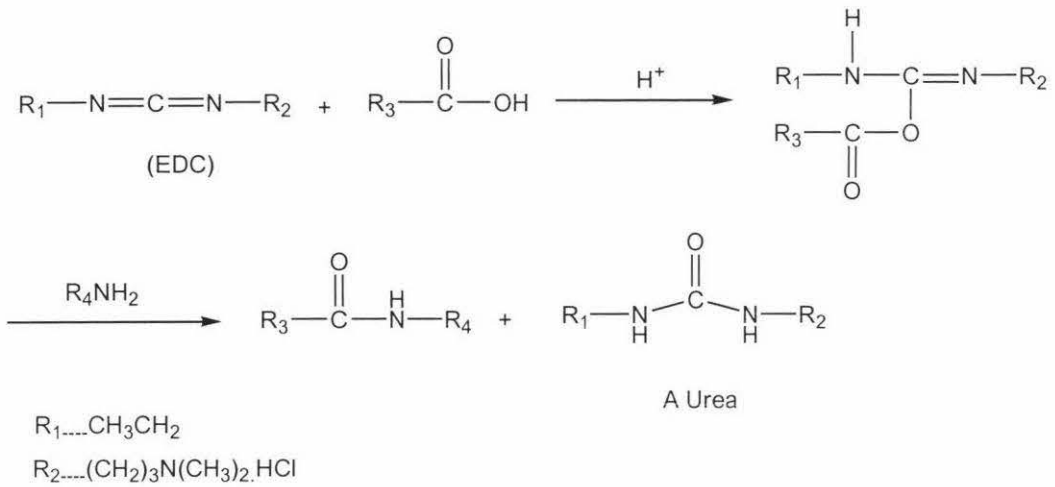

Scheme 2.6. EDC coupling reaction

EDC reacts with a carboxylic acid to form an active *O*-acylisourea intermediate, which is subsequently attacked by the incoming amino group in the reaction mixture. An EDC by-product is released as a soluble urea derivative after displacement by the nucleophile. The intermediate in this synthesis does not need to be isolated, and both steps take place at room temperature, to produce amides in good yield.[69]

In the current work the use of coupling reagents proved unsuccessful, giving only lactobionic acid **(45)** or one of its salts. The likely reason for this failure is that the carboxylic group is at the C-1 position of a glucose derivative. The hydroxy group attached at C-5 (and possibly at C-6) can compete with an "external" nucleophile group in attacking the acyl carbon atom, leading to a lactone **(46)** product.

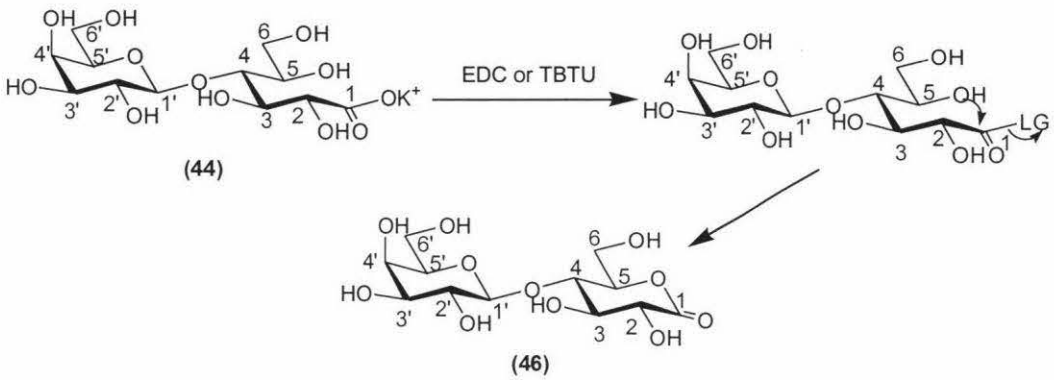

Scheme 2.7. Coupling reaction from potassium lactobionate to lactone

Although the lactone itself is effectively an "activated" intermediate, it is vulnerable to hydrolysis in situ, leading back to the starting materials. Although hydroxyl groups are generally less nucleophilic than amino groups, reactions with the EDC coupling reagent are best carried out at pH 4-5 (to prevent overly-rapid hydrolysis of the activated intermediate), and at this pH the amino group is partially unprotonated and therefore nucleophilic. Furthermore, the concentration of amino groups in the dilute solution is likely to be much lower than the effective concentration of the C-5 hydroxyl at the reacting centre. Since the added amino group cannot effectively compete with the intramolecular reaction, it was decided to form lactobionic acid **(45)** then lactone **(46)**, and then to react this species with the appropriate amino group.

Lactobionic acid (45)

Potassium lactobionate **(44)** was converted to the free acid by treatment with cationic ion exchange resin. The proton NMR spectrum of freshly prepared lactobionic acid indicated absence of starting material, but the presence of two new β-galactoside products, both retaining the anomeric doublet at ca. 4.5ppm. One of the compounds was identified as the δ-lactone **(46)** (cyclic) form, on the basis of the appearance of a doublet at 4.21ppm and a triplet at 4.09ppm, both exhibiting the large coupling constants (J=10.2Hz and J=9.1Hz respectively) expected from ring protons in diaxial relationships about a cyclic system. A doublet of doublets observed at 4.16ppm was assigned to the lactobionic acid **(45)** (acyclic form) because it has small coupling constants (J=4.5Hz and J=3.2Hz). The intensities of these peaks varied in a manner consistent with the ratio of products in the mixture.

The lactone **(46)** to lactobionic acid **(45)** ratio in the original NMR sample was monitored over the course of nine days (Figure 2.1).

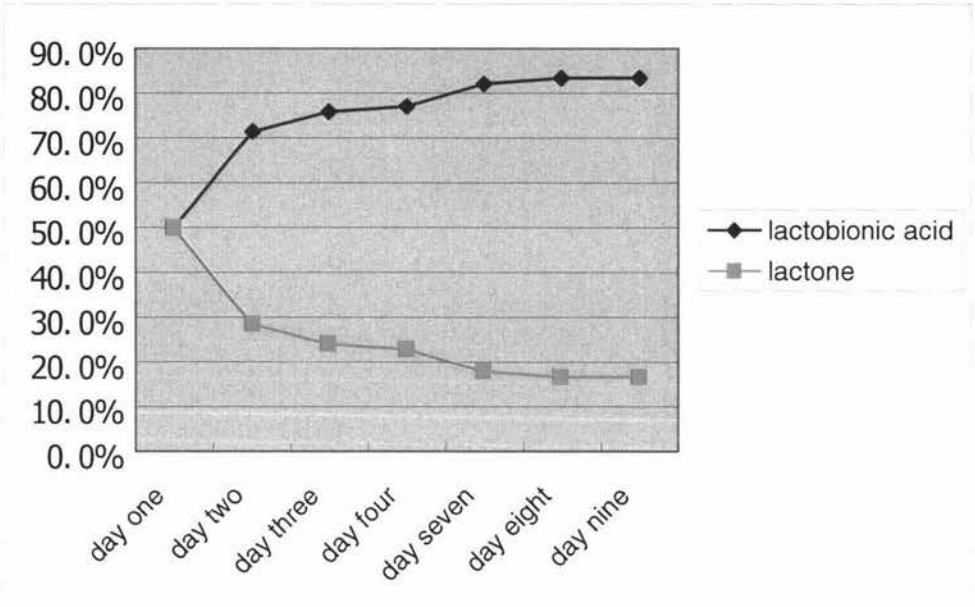

Figure 2.1. Starting point - fresh lactobionic acid **(45)** in D_2O

As indicated, the sample of freshly prepared lactobionic acid **(45)** contained roughly fifty percent lactone **(46)** initially. Over the course of several days standing at RT in D_2O, the proportion of lactobionic acid **(45)** slowly increased to an apparent equilibrium figure of nearly 85%. Since the product ratio was observed to change slowly in D_2O, the exact initial product ratio is in doubt, but the ratio of products obtained through further reactions on the lactone **(46)** preparation supports the presence of a mixture initially. This indicated that the lactobionic acid **(45)** – lactone **(46)** conversion was reversible, with the position of equilibrium favouring the free acid form.

Lactone (46)

Several solvents were used in attempts to strip water from solutions of lactobionic acid **(45)**, and drive the equilibrium toward the lactone **(46)**. Repeated evaporation of methanol from a lactobionic acid **(45)** solution resulted in a mixture that still contained significant amounts of the free acid, along with the corresponding methyl ester and lactone **(46)** forms (see Figure 2.2 below). The presence of a methyl ester was indicated by the appearance of a new doublet at 4.6ppm, with the small coupling constant (J=3.27Hz) expected for an acyclic system, assigned to 2-H and also a 3-

proton singlet for OMe at 3.8ppm. 2-Methoxyethanol was investigated next, since its high boiling point (123°C) was expected to improve solubilisation of the acid, but again mixtures of lactobionic acid (**45**), lactone (**46**), and ester were obtained. In order to avoid ester formation, *tert*-butanol was chosen. But although no *t*-butyl ester was observed in this case, the ^{1}H NMR spectrum still indicated the presence of two compounds, the lactone (**46**) and lactobionic acid (**45**).

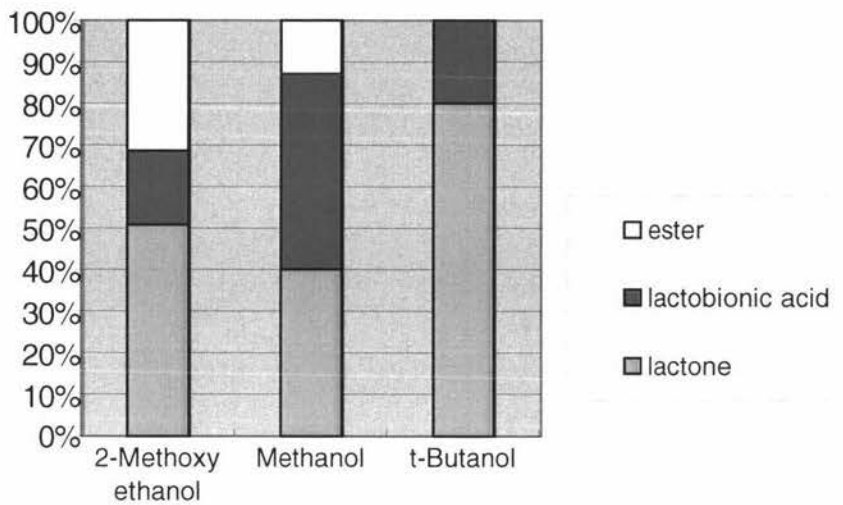

Figure 2.2. Different percentage of lactone (**46**) in different solvents

This graph indicates that *t*-butanol gave the highest percentage of lactone (**46**) (80%) of these three different solvent systems; the other twenty percent was lactobionic acid (**45**), with no ester present. 2-Methoxyethanol gave 51% lactone (**46**), 18% lactobionic acid (**45**) and 32% 2-methoxyethyl ester. Not surprisingly methanol, a primary alcohol with the lowest boiling point of the three, gave only 40% lactone (**46**), 47% lactobionic acid (**45**), and 13% methyl ester. The ratio of products in the latter mixture in D_2O solution was monitored over several days (Figure 2.3).

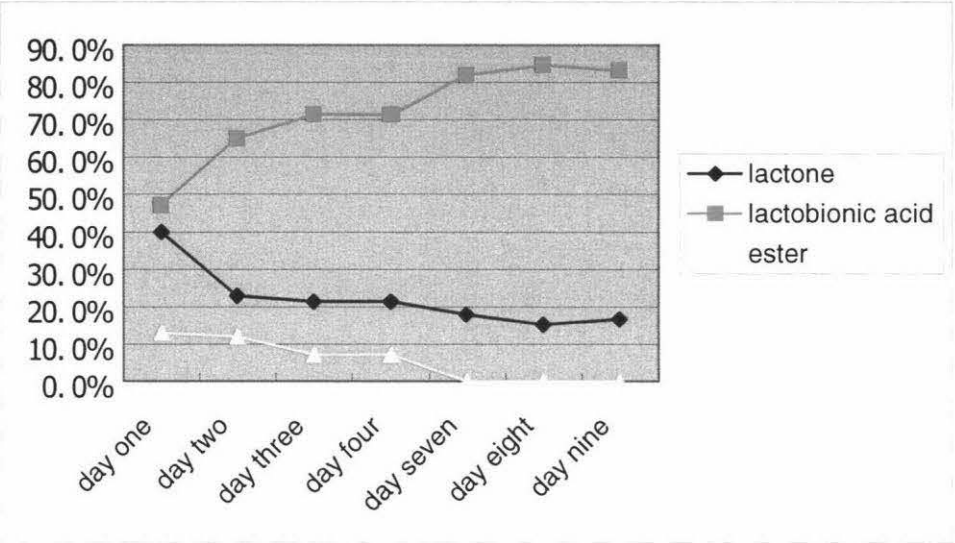

Figure 2.3. Starting point - fresh lactone **(46)** in MeOH in D_2O

Once more, an equilibrium mixture of about 85% lactobionic acid **(45)** to 15% lactone **(46)** was established after about a week standing in D_2O at RT (Figure 2.4).

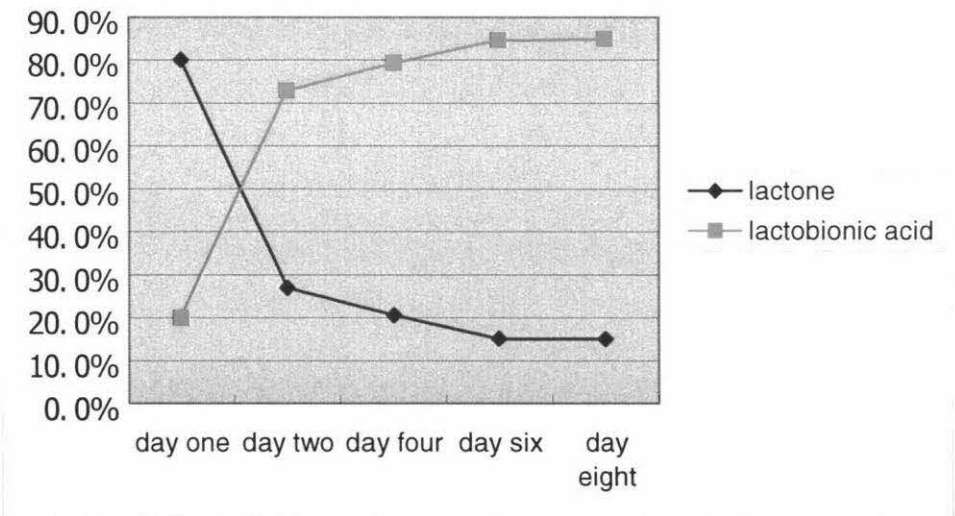

Figure 2.4. Starting point - fresh lactone **(46)** in *t*-butanol in D_2O

In the case of the mixture produced from evaporation of t-butanol, no ester was present initially. Again, an equilibrium ratio of about 85% lactobionic acid **(45)** to 15% lactone **(46)** was established.

In order to test amide formation with lactone **(46)**, allylamine was chosen as a readily available volatile amine. Excess allylamine was added to a mixture of lactone **(46)** and lactobionic acid **(45)** in methanol solution and refluxed. (Scheme 2.8).

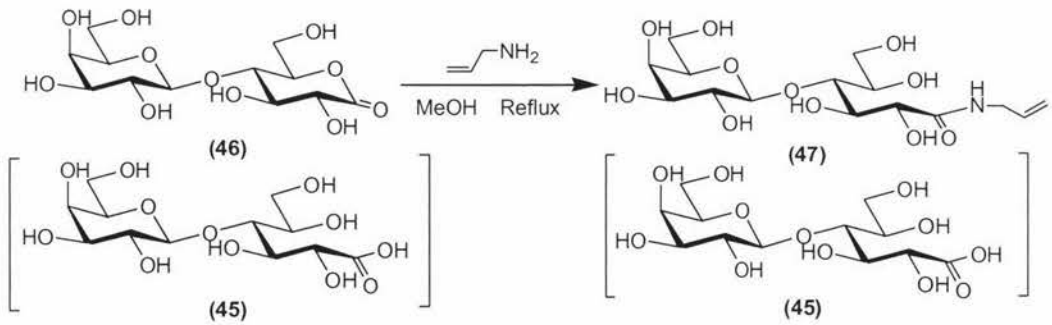

Scheme 2.8. Reaction of allylamine with lactone **(46)**

After completion of the reaction, excess allylamine was removed by evaporation, the products were the desired lactose-allyl amide **(47)** and unreacted lactobionic acid **(45)**. The allyl peaks present at 5.95ppm, 5.16ppm and 5.05ppm all display multiple coupling patterns. In order to test the reactivity of this double bond, different methods were used to polymerize this compound.

In aqueous solution, potassium persulfate was used as the initiator of radical polymerization. In organic solvent, AIBN played the same role. However, in the course of repeated attempts to effect the polymerization, the characteristic peaks due to the terminal double bond of the starting material were still present in the proton NMR spectrum of the reaction mixture, indicating that the radical polymerization had not taken place.

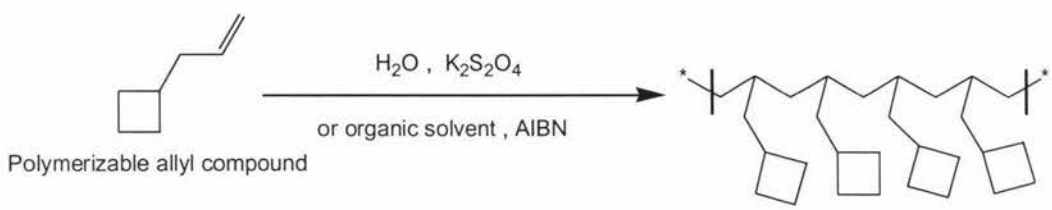

Scheme 2.9. Polymerization of allyl double bond

N-vinylpyrrolidone (NVP) was used as a test radical initiator for these reactions. Using the same reaction conditions, the reaction proceeded to completion, as

evidenced by the loss of double bond signals from the NMR spectrum of the crude product mixture. As a result, it was concluded that the double bond of the lactose-allyl amide **(47)** was not active enough to perform the polymerization under the conditions used above. Therefore the synthesis of a lactose acrylate was pursued, in the expectation that a monomer bearing this more reactive double bond would polymerize more readily.

Acryloyl chloride, which readily undergoes nucleophilic substitution reactions, was selected as the acryloyl donor. To couple the acryloyl group to lactone **(46)**, a diamine was to be used, to result in the formation of a lactose – acryloyl diamide.

Firstly hexamethylenediamine was reacted with acryloyl chloride, but it proved difficult to accomplish mono-acrylation despite the use of various reaction conditions. The pKa of the amino groups of hexamethylenediamine are too similar to allow for regioselective reaction through careful control of pH. Ethylenediamine, on the other hand, has pKa's of 10.08 (20 °C) and 6.99 (20 °C), and therefore it is easy to control the mono-reaction of ethylenediamine by adjusting the pH (Scheme 2.10).

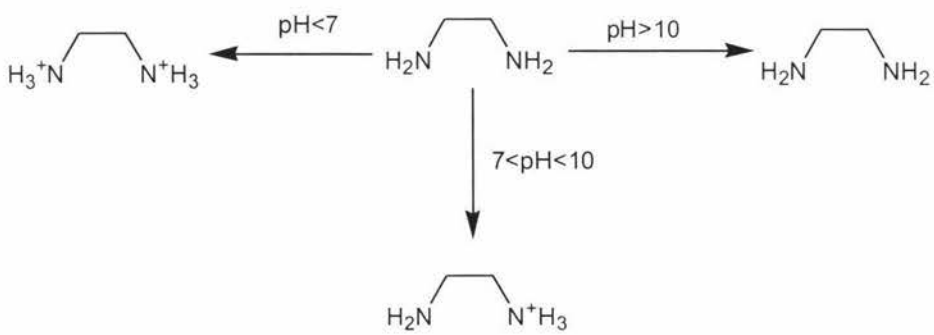

Scheme 2.10. Behaviour of ethylenediamine at different pH conditions

At pH 7, one amino group will be protonated (and hence non-nucleophilic), while the other will remain uncharged and will react to give mono-acryloyl ethylenediamine.

2.2 Preparation of Monomer one (51)

Preparation of mono-*N*-Boc-ethylenediamine **(48)**

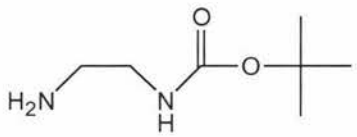

(48)

An eight fold excess of ethylenediamine was reacted with one equivalent di-tert-butyldicarbonate in DCM. After the reaction was complete, water was slowly added and the mixture stirred for 15 minutes. The aqueous phase was separated. Water was added to the organic layer and the pH adjusted to 1.5 with concentrated HCl, stirred for a 10 minutes and the organic phase removed. DCM was added to the aqueous phase which was then adjusted to pH 12 with 28% NaOH, stirred for 10 minutes. The organic phase was then separated. Finally the water phase was extracted with DCM. The DCM phases were combined and dried over $MgSO_4$. The solvent was evaporated under reduced pressure, and the residue was dried *in vacuo*. However after these purification steps the yield of mono-Boc-ethylene diamine was low, about 20%. Therefore the workup steps were deleted in future experiments and the reaction mixture was evaporated under reduced pressure after the reaction. The NMR and mass spectra indicated that the purity of mono-Boc-ethylene diamine was reasonable without the purification steps. ^{1}H NMR spectrum showed that only one broad single hydrogen peak from amide at 5.15ppm, methylene group next to the amide exhibited broad doublet (J=5.67Hz) at 3.11ppm, because the special effects from bulky Boc group distort the original triplet and made the peaks broader. Another methylene group next to amino group displayed a normal triplet (J=5.9Hz) at 2.74ppm. One single peak for the Boc group showed at 1.39ppm. The integrals of each peak showed the right number of protons in this molecule, furthermore no other signals were observed in proton NMR spectrum. The IR spectrum of this product exhibited strong absorptions at 3357.5cm^{-1}and 1692.8cm^{-1}, that were assigned to N-H stretching and carbonyl stretching respectively. Finally the correct parent ion (M+1=161) was observed in the ES (+) mass spectrum, and no parent ions were observed for ethylene

diamine and di-Boc-ethylenediamine. Therefore all these facts gave evidence that mono-Boc ethylenediamine **(48)** was successfully synthesized.

Preparation of *N*-Acryloyl-*N*-Boc-ethylenediamine **(49)**

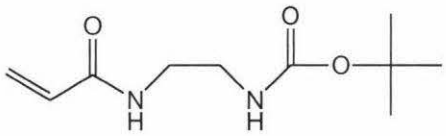

(49)

Mono-Boc-ethylenediamine **(48)** was reacted with acryloyl chloride in the presence of DIEA in an ice-bath. After the reaction finished, the mixture was washed by 0.1M HCl to get rid of unreacted compounds and DIEA. TLC (EtOAc) indicated three compounds in the mixture. Therefore the mixture was purified by column chromatography (SiO_2, hexane/EtOAc). The first compound came out very quickly at 50:50 (v/v) hexane:ethyl acetate, the second compound came out between 20:80 (v/v) and 10:90 (v/v) hexane:ethyl acetate; the third one came out directly with ethyl acetate. The proton NMR spectrum confirmed that the second compound was *N*-acryloyl-*N*-Boc-ethylenediamine **(49)**, with R_f 0.448 (EtOAc). In the proton NMR spectrum, two broad single hydrogen peaks of amide showed at 6.59ppm and 5.07ppm. The methylene of the double bond exhibited multiple peaks at 6.2ppm, C**H** of the double bond displayed a doublet of doublets coupling pattern (J=10.3Hz, J=1.2Hz) at 5.65ppm. The methylene group next to acryloyl group showed a doublet of doublets coupling pattern (J=11Hz, J=5.3Hz) at 3.45ppm. The methylene group beside the Boc group showed a broad triplet coupling pattern (J=5.5Hz) at 3.33ppm. The Boc group showed a single peak at 1.44ppm. The IR spectrum showed new peaks at 3076.7cm^{-1} assigned to C-H stretching of alkene, at 1662.8cm^{-1} assigned to stretching of the carbonyl conjugated to the double bond, and at 1628.9cm^{-1} assigned to conjugated double bond stretching. N-H stretching and carbonyl stretching for the ester still presented at 3301.6cm^{-1} and 1696.0cm^{-1}. Finally the correct parent ion (M+1=215) was observed in ES (+) mass spectrum.

Preparation of *N*-Acryloyl-ethylenediamine **(50)**

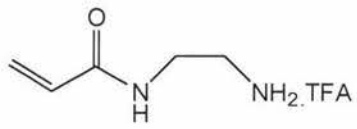

(50)

N-Boc-*N*-acryloylethylenediamine **(49)** was deprotected in a mixture of DCM and trifluoroacetic acid. TFA combines with the amino group to form a TFA salt. *N*-Acryloyl-ethylene diamine **(50)** was usually obtained as a colorless oil. In the proton NMR spectrum, the protons from the double bond still showed at 6.24ppm and 5.78ppm. The methylene group next to the acryloyl group exhibited a triplet coupling pattern (J=5.85Hz), and the methylene group beside the amino group showed triple coupling pattern (J=5.78Hz). The singlet peak of Boc group had disappeared totally. The carbonyl stretching for the urethane (1696.0cm^{-1}) had disappeared from the IR spectrum. There was little other change in the IR spectrum from the starting material. Finally the correct parent ion (M+1=115) was observed in the ES (+) mass spectrum and the parent ion (M+1=215) of *N*-Boc-*N*-acryloylethylene diamine **(49)** disappeared from the ES (+) mass spectrum.

Monomer one (51)

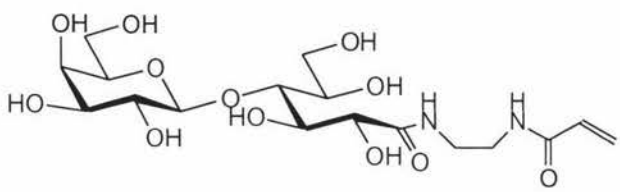

(51)

N-Acryloyl-ethylenediamine **(50)** was reacted with a mixture of lactone **(46)** and lactobionic acid **(45)** under DIEA basic conditions in MeOH. *N*-acryloyl-ethylenediamine **(50)** can combine with TFA during the deprotection process making the free amino group non-nucleophilic. DIEA is added to release the amino group of *N*-acryloyl-ethylenediamine **(50)**. After the reaction was completed the excess DIEA was removed by cationic ion exchange chromatography. However Monomer one **(51)**

was still mixed with lactobionic acid **(45)** as shown by the ES (-) mass spectrum with the parent ion of lactobionic acid **(45)** showing at 357 (M-1). Because the polarity between the monomer one **(51)** and lactobionic acid **(46)** was very similar, it was difficult to separate them by column chromatography (SiO_2, 85:30:10 v/v, ethyl acetate: methanol: water). Reverse phase HPLC was used for the separation. Lactobionic acid **(45)** firstly came off the column at the 3.6% solvent B. Monomer one **(51)** started to elute at the 5% solvent B just after the lactobionic acid **(45)** peak had just returned to the baseline. The monomer one **(51)** elution was complete at the 9% solvent B.

The acryloyl double bond displayed at 6.24ppm and 5.77ppm in the proton NMR spectrum. 1'-H exhibited a doublet (J=7.85Hz) at 4.46ppm indicating retention of the galactose residue in its cyclic acetal form. The 2-H signal moved from 4.16ppm to 4.31ppm due to the formation of the amide bond next to 1-H that changed the chemical environment of 2-H and made it move to down field, but the doublet coupling pattern and coupling constant (J=2.7Hz) did not change much. Other protons on lactose were not affected by the addition of acryloyl ethylenediamine. However one new broad triplet signal appeared at 3.35ppm in the spectrum that can be assigned to the two methylene groups of ethylenediamine. The two methylene groups were next to amide groups and hence had similar environments and their chemical shifts were almost the same in the proton NMR spectrum. The two triplets overlapped together and produced a broad triplet in the proton NMR spectrum.

The ^{13}C NMR spectrum exhibited exactly seventeen carbon signals, and no TFA carbon peaks appeared in the spectrum. Two signals in the carbonyl region at 174.6ppm and 168.8ppm confirmed two amide bonds existed in the molecule. Two signals in the unsaturated carbon region at 129.9ppm and 127.4ppm (DEPT carbon NMR spectrum) were assigned to CH and CH_2 respectively. One signal in the anomeric region (103.4ppm) was assigned to 1'-C. Methylene groups of 6-C and 6-C' on lactose and two methylene groups of ethylene diamine were all separated by DEPT from other signals, 61.9ppm and 61.0ppm assigned to 6-C and 6-C'. Two methylene groups on diamine were recognized at 38.6ppm and 38.4ppm. Other carbon signals on lactose were all at the correct position in the carbon NMR spectrum, 80.9ppm for 4-C, 75.3ppm for 5'-C, 72.4ppm 72.3ppm 71.4ppm 71.0ppm 70.4ppm for 2-C 2'-C 3-C 3'-

C 5-C, 68.6ppm for 4'-C. Finally the IR spectrum of product exhibited a strong absorption at 1657cm^{-1} that was assigned to the carbonyl stretching. The correct parent ion (M+1=455) was observed in ES (+) mass spectrum.

2.3 Preparation of Monomer two (57)

Lysine **(52)**

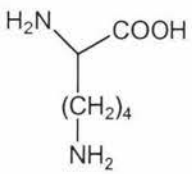

(52)

In order to investigate monomer construction from a different angle, lysine **(52)** was selected as the basic building block. Firstly lysine **(52)** has two amino groups in the molecule and has longer alkyl chain than ethylene diamine between the two amino groups that will exhibit quite different biological characteristics in the polymer. Secondly lysine **(52)** is a naturally occurring amino acid. Mammalian proteins are polyamides and their monomeric units are commonly selected from twenty different α-amino acids. Cells use the different α-amino acids to synthesize the proteins. Therefore putting an amino acid in a polymer should be of interest in tissue engineering.

Preparation of N^{ε}-Boc-L-lysine **(53)**

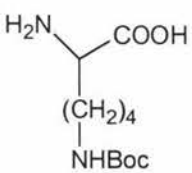

(53)

N^{ε}-Boc-lysine **(53)** was synthesized via the formation of a metal complex. Firstly $CuSO_4.5H_2O$ was added to L-lysine.HCl in $NaHCO_3$ (2M) aqueous alkaline solution. The copper complex formed between α-amino group and carboxylic acid was then

treated with a di-tert-butyldicarbonate acetone solution to react with the free ε-amino group. The N^{ε}-(Boc)-L-lysine copper complex was isolated as a blue precipitate. The blue residue after filtration was treated with water and 8-hydroxyquinoline then stirred at room temperature for 5 hours. The removal of the copper from the complex was monitored by the color change of the solution from blue to white. The mixture was filtered, the white solid was dissolved in water and stirred for a day. This solution was filtered again, and the filtrate was washed with ethyl acetate, then the aqueous layer was freeze dried in vacuo. A white solid was obtained.

The ^{1}H NMR spectrum of the product displayed a triplet (6.13Hz) at 3.70ppm that was assigned to the α-C**H**, the proton next to the α-amino group and carboxylic acid group. Therefore the signal exhibited at the most down field position in the NMR spectrum and it was also next to a methylene group and displayed as a triplet in the spectrum. The signal at 3.07ppm, exhibited a triplet (J=6.68Hz) and was assigned to the methylene group that was next to the amine-Boc group. The COSY spectrum showed strong clear correlations between these protons in the molecule. A multiplet at 1.85ppm was assigned to the methylene group that was next to the CH (C**H**$_2$CH), because this methylene group not only couples with the C**H** group but also the C**H**$_2$ group next to it, hence a multiplet coupling pattern. The signal at 1.53ppm was assigned to C**H**$_2$CH$_2$NHBoc, and due to its multiple coupling behaviour this signal displayed a multiplet as well. Integration indicated eleven protons at 1.43ppm, that were assigned to the three methyl groups of the Boc group that exhibited big singlet and one methylene group from the lysine backbone that showed multiplet overlapped with Boc signal. No other extra signals were observed in the spectrum and the integrals for each signal were correct. Finally the correct parent ions (M+1=247, M-1=245) were observed in ES (+) and ES (-) mass spectrum.

Preparation of N^{α}-Acryloyl-N^{ε}-Boc-L-lysine **(54)**

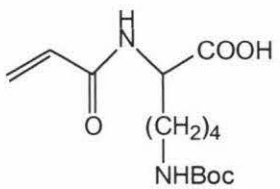

(54)

One equivalent of N^{ε}-Boc-L-lysine **(53)** was dissolved in a mixture of aqueous NaOH and CH_3CN, 1.2 equivalents of acryloyl chloride were added dropwise and the reaction stirred for 2hrs. After the reaction was completed, the solution was acidified to pH 1 and extracted with ethyl acetate three times. The excess acryloyl species and unreacted N^{ε}-Boc-L-lysine **(53)** remained in the aqueous phase. The product N^{α}-acryloyl-N^{ε}-Boc-L-lysine **(54)** was isolated from the ethyl acetate phase. The ethyl acetate extracts were combined and dried over $MgSO_4$. The solvent was evaporated under reduced pressure to give a white solid.

Preparation of N^{α}-Acryloyl-N^{ε}-Boc-L-lysine-butylamide **(55)**

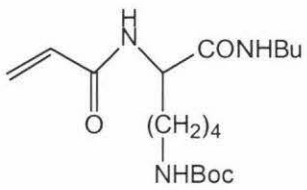

(55)

In order to link the lactone **(46)** through an amide bond, the Boc group had to be removed from N^{α}-acryloyl-N^{ε}-Boc-L-lysine **(54)**. However because the carboxylic acid group in the lysine **(52)** is unprotected, the ε-amino group could in principle also attack that carbonyl carbon of lysine to form a seven-membered ring. This then would be instead of attacking the carbonyl carbon of the lactone **(46).** Even though the seven-membered ring is not favored for ring closure type, the chance still exists. Therefore the carboxylic acid group was protected before deprotecting the ε-amino group. At this stage, coupling reagents EDC and NHS were used with *n*-butylamine as the nucleophile reacting with the carboxylic acid to form the amide bond.

One equivalent N^{α}-acryloyl-N^{ε}-Boc-L-lysine **(54)** mixed with 1.1 equivalents of EDC.HCl and N-hydroxysuccinimide dissolved in DCM. Two hours later, *n*-butyl amine was added and reacted overnight. The solvent was removed by evaporation and the mixture purified by column chromatography (SiO_2, hexane/EtOAc). The gradient phase started at 50:50 (v/v) hexane:ethyl acetate with the product eluting at 20:80 (v/v) hexane:ethyl acetate. TLC in ethyl acetate gave a product R_f of 0.48.

The ^{1}H NMR spectrum of the product exhibited a multiplet and a doublet of doublets (J=10.05Hz and J=1.55Hz) at 6.25ppm and 5.67ppm, assigned to acryloyl double bond protons C**H**$_2$ and C**H** respectively. The α-C**H** linked to the amino and carbonyl groups displayed a doublet of doublets (J=14.05Hz and J=7.8Hz) at 4.55ppm. The C**H**$_2$ on the n-butyl backbone beside the amide group displayed a multiplet at 3.21ppm. The C**H**$_2$ on the lysine backbone next to the urethane gave a broad multiplet at 3.09ppm. Other methylene groups from the butyl and lysine backbones displayed a broad multiplet from 1.56ppm to 1.26ppm, and a singlet at 1.44ppm, assigned to the Boc group. A triplet (J=7.3Hz) signal at 0.91ppm was assigned to methyl group from the butyl backbone.

Further data for this molecule were provided by the ^{13}C NMR spectrum, which showed three signals in the carbonyl region at 172.2ppm, 165.8ppm and 156.1ppm. Two signals displayed in the unsaturated carbon region at 130.7ppm and 126.5ppm, and were distinguished by the ^{13}C DEPT spectrum and assigned to the **C**H and **C**H$_2$ carbons respectively. The **C**-(CH$_3$)$_3$ from the Boc group displayed at 78.9ppm. The α-**C**H of HN**C**HCO, the CH$_3$ groups of the C-(**C**H$_3$)$_3$ and the CH$_3$ of CH$_2$**C**H$_3$ all displayed cleanly from other signals in the carbon DEPT NMR spectrum at 53.1ppm, 28.4ppm and 13.7ppm. With the help of HMQC and DEPT, the **C**H$_2$ of **C**H$_2$NHBoc, CHCONH**C**H$_2$ and CH**C**H$_2$ were distinguished from the other carbons of the methylene groups at 40.1ppm, 39.2ppm and 32.3ppm. The last four carbon signals of **C**H$_2$ displayed at 31.3ppm, 29.4ppm, 22.7ppm and 19.9ppm. They were so close to each other that it was difficult to separate them.

The IR spectrum of this product exhibited strong absorptions at 3287cm^{-1}, 1693.3cm^{-1}, 1650.2cm^{-1} and 1624.9cm^{-1} assigned to N-H stretching, carbonyl stretching of ester, carbonyl stretching conjugated with a double bond, and C=C stretching of conjugated double bonds respectively. Finally the correct parent ion (M+1=356) was observed in the ES (+) mass spectrum.

Preparation of N^{α}-Acryloyl-L-lysine-butylamide **(56)**

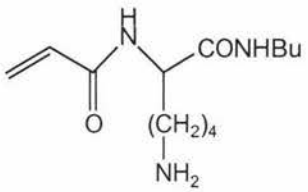

(56)

The Boc group was removed from fully protected lysine with a 1:1 (v/v) mixture of DCM and TFA. The ^{1}H NMR spectrum showed that the single peak for the Boc group at 1.44ppm had disappeared totally, and the multiplet peaks for the CH_2 beside Boc group at 3.09ppm had moved to 3.00ppm and displayed as a triplet (J=7.35Hz). The ^{13}C spectrum produced only two signals in the carbonyl region (173.63ppm and 168.47ppm). The signals for the Boc group (**C**-$(CH_3)_3$ and C-(**C**$H_3)_3$) at 78.9ppm and 28.4ppm had disappeared. The methylene carbon (**C**H_2) beside Boc (urethane) group at 40.1ppm had moved to 39.05ppm. Finally the correct parent ion (M+1=256) was observed in ES (+) mass spectrum, and parent ion (M+1=356) disappeared.

Monomer two (57)

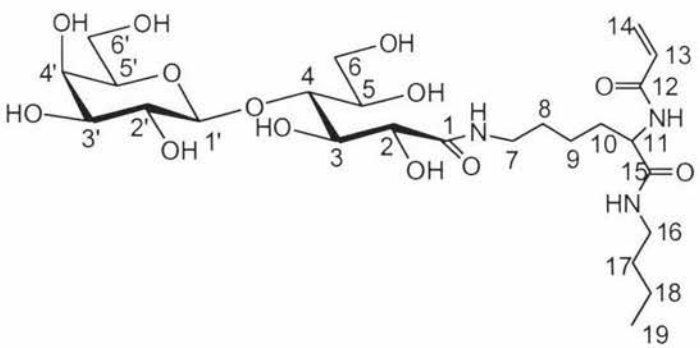

(57)

Next, the free ε-amino group was reacted with the lactone **(46).** N^{α}–Acryloyl-L-lysine butylamide **(56)** was mixed with 1 equivalent mixture of lactone **(46)** and lactobionic acid **(45)** with DIEA in a MeOH solution overnight. DIEA provided basic reaction conditions to ensure that the amino group was free of TFA. After the reaction was complete, the solvent was evaporated. This crude product was checked by MS. The

ES (-) mass spectrum gave the expected parent ion (M-1=594) as well as the parent ion (M-1=357) for lactobionic acid **(45)**, which means lactone **(46)** reacted with N^{α}–acryloyl-L-lysine butylamide **(56)** completely and lactobionic acid **(45)** did not get involved in the reaction. In other words, the product of Monomer two was still mixed with unreacted lactobionic acid **(45)**.

Reversed phase HPLC was again used to remove the lactobionic acid **(45)** from the product. As with the separation of Monomer one **(51)**, the lactobionic acid **(45)** came out first and Monomer two **(57)** eluted later. This separation was more efficient than the previous Monomer one **(51)** separation. This may be because the Monomer two **(57)** has more alkyl groups than Monomer one **(51)**. This would make the polarity difference between Monomer two **(57)** and lactobionic acid **(45)** greater than that between Monomer one **(51)** and lactobionic acid **(45)**. The final compound was a white solid. TLC in ethyl acetate, methanol and water (85: 30: 10 v/v) gave a product with R_f of 0.48. The parent ion (M-1=357) of lactobionic acid **(45)** had disappeared in the ES (-) mass spectrum.

The ^{1}H and ^{13}C NMR spectra both confirmed the correct structure for this molecule. The acryloyl double bond displayed at 6.2ppm and 5.7ppm in the proton NMR spectrum. The 1'-H exhibited a doublet (J=7.7Hz) at 4.5ppm indicating retention of the galactose residue in its cyclic acetal form. The signal of the 2-H moved from 4.16ppm to 4.3ppm due to the formation of the new amide bond next to 1-H. This changed the chemical environment of 2-H and made it move downfield, but the doublet coupling pattern and coupling constant (J=2.76Hz) did not change much. Other protons on the lactose moiety were not affected by the addition of the *N*-acryloyl-L-lysine *n*-butylamide **(56)** group. In other words, signals from those protons did not change in the spectrum. Most of the signals of *N*-acryloyl-L-lysine *n*-butylamide **(56)** did not change in the proton NMR spectrum. The only one that did change was the C**H**$_2$ beside the new amide bond that moved from 3.0ppm to 3.2ppm. With the help of COSY, ^{13}C, DEPT and HMQC spectra, the other methylene groups of lysine **(52)** and butyl backbone could be separated, multiple signals at 3.14ppm, 1.73ppm, 1.50ppm, 1.42ppm, 1.34ppm, 1.27ppm assigned to 16-H, 10-H, 8-H, 17-H, 9-H, 18-H respectively. A triplet (J=7.35Hz) at 0.82ppm was assigned to the C**H**$_3$.

The ^{13}C spectrum displayed three signals in the carbonyl region at 174.6ppm, 174.4ppm and 169.0ppm that indicated a new amide bond formed between the free amino group and lactone, and confirmed three amide bonds existed in the molecule. Two signals in the unsaturated carbon region at 129.1ppm and 128.0ppm. DEPT carbon NMR spectrum gave evidence for separating them and assigning them to the **C**H and **C**H_2 respectively. One signal in the anomeric region (104.3ppm) was assigned to 1'-C. Ten signals in the lactose region (from 81.3ppm to 61.6ppm), were assigned to the carbons from lactose. The remaining final nine signals in alkyl region (from 54.6ppm to 13.2ppm) were assigned to carbons from the lysine **(52)** and butyl backbones. The number of carbons in the molecule was exactly the same as number of signals in the carbon spectrum, therefore Monomer two **(57)** was synthesized successfully and was pure.

2.4 Preparation of Monomer three (58)

When working with the lactone **(46)** it was always mixed with lactobionic acid **(45)**, however potassium lactobionate **(44)** was readily purified as a crystalline solid. Use of this pure starting material to react with amino groups should simplify further product purification steps and increase the yields. When using potassium lactobionate **(44)** the main functional group is of course the carboxylic acid. Therefore coupling reagents such as EDC and DCC were considered. However, because the problem of the intra-molecular ring closure reaction was preferred over "external" nucleophilic substitution, direct use of potassium lactonate **(44)** was thought to be unadvisable. Therefore the hydroxyl groups of lactose were blocked to hopefully avoid this problem. Acetyl groups were chosen to block the hydroxyl groups of the carbohydrate group.

Potassium lactobionic acid **(44)** was mixed with a solution of pyridine and acetic anhydride and reacted for four days. After the reaction was completed, the mixture was poured into a ice-cold saturated sodium chloride solution. Gummy lumps came out of solution. The lumps were dissolved in DCM and dried over $MgSO_4$. The solvent was removed by rotary evaporator and dried *in vacuo*. The product was purified by column chromatography (SiO_2, 50:50 (v/v), hexane: ethyl acetate).

Monomer three (58)

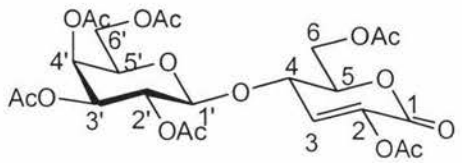

(58)

In the proton NMR spectrum, firstly, one doublet at 6.68ppm was noted in unsaturated proton region and represented one hydrogen (3-H). Secondly, six singlets for the acetyl groups from 2.27ppm to 1.99ppm were noted. In fact, potassium lactobionate **(44)** has eight hydroxyl groups, so there should have been eight single signals of acetyl groups in this range, and there should have been no signal at 6.68ppm. From these facts it can be concluded that a new compound formed during this reaction and this new compound must contain a double bond in the molecule. The only possible position to form double bond was at 2-H, because carbonyl group makes the 2-H more acidic than normal, so it could be easily eliminated in presence of a base, such as pyridine, in the acylating solution. The initially formed acyl group at the 3-C atom would make a good leaving group for elimination with pyridine. Therefore the double bond formed between 2-C and 3-C. Except for the now missing 3-C acetyl group, there still should have been seven acetyl groups in the molecule. The most likely possibility for the other missing acetyl group would be at the 5-C position, i.e. the intra-molecular ring closure reaction had occured instead of the acylation reaction. In this case, after elimination and ring closure, the new compound would have six acetyl groups in the molecule Schme 2.11).

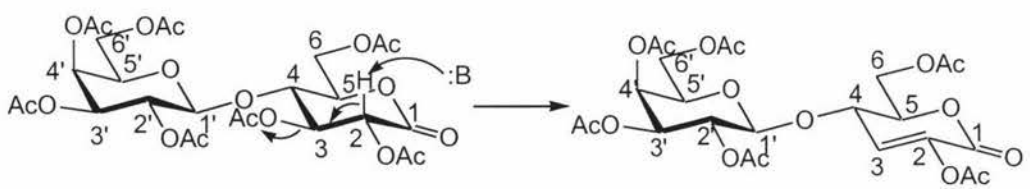

(58)

Scheme 2.11. Mechanism for the elimination reaction in the acetylation of lactobionic acid

Because the effects of acetyl groups in the molecule in the proton NMR spectrum, all signals shifted downfield. A doublet (J=2.33Hz) at 6.68ppm was assigned to 3-H, because it only coupled to 4-H. The equatorial 4'-H did not couple to 5'-H and only weakly coupled to 3'-H giving a small doublet (J=2.6Hz). The signal at 5.23ppm displayed a large doublet of doublets (J=10.4Hz, J=7.93Hz), assigned to 2'-H, because 2'-H is coupled to 1'-H and 3'-H and has trans-diaxial relationships with 1'-H and 3'-H, and so produces a large doublet of doublets (J=10.4ppm J=7.93ppm). The 1'-H coupled only to the 2'-H and displayed a doublet. From the COSY spectrum, the doublet signal (J=7.9Hz) displayed at 4.65ppm and was assigned to 1'-H. The 3'-H at 5.03ppm displayed a doublet of doublets (J=10.4Hz, J=3.4Hz), because 3'-H has trans-diaxial relationship with 2'-H that gives a large coupling constant, and is equatorial and coupled with 4'-H to gave a small coupling constant.

The COSY spectrum showed strong clear correlations from 3-H to 6-H. Because there is no hydrogen at 2-C due to the formation of the double bond, 3-H only coupled to 4-H, so a doublet of doublets (J=9.4Hz, J=2.3Hz) at 4.70ppm was assigned to 4-H. This was because 4-H is not only equatorial to 3-H and gave a small coupling constant (J=2.3Hz), but it is also trans-diaxial with 5-H and gave a large coupling constant (J=9.4Hz). 5-H displayed a multiplet at 4.62ppm due to multiple coupling to 4-H and 6-H_A and 6-H_B. After acetylation, the 6-position and 6'-position hydrogens behave in the NMR differently. The acetyl groups instead of hydroxyl groups, where the C-O bonds between the acetyl group and oxygen rotate, produces two hydrogens located in different chemical environments. These two hydrogens display different signals in the proton spectrum. Usually this coupling system is called an ABX coupling system. (Scheme 2.12)

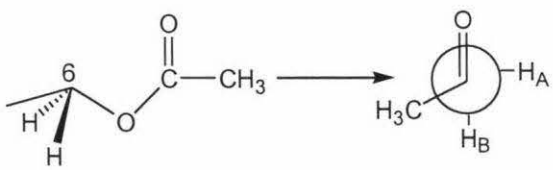

Scheme 2.12. ABX coupling system

When the hydroxyl groups are unprotected, these two hydrogens show no difference when the bond rotates. 5-H coupled to 6-H_A and 6-H_B, a doublet of doublets (J=12.48Hz, J= 2.49Hz) at 4.36ppm was assigned to 6-H_A. 6-H_B displayed a doublet of doublets as well, but it overlapped with other signals and could not be separated clearly from 4.26ppm to 4.13ppm. 6'-H_A displayed clearly a doublet of doublets (J=11.35Hz, J=6.24Hz) at 4.12ppm. 6'-H_B displayed at the same range as 6-H_B from 4.26ppm to 4.13ppm. Therefore signals of 6-H_B and 6'-H_B overlapped together and made them look like multiple signals. 5'-H coupled to 6'-H_A and 6'-H_B showed a triplet (J=6.58Hz) at 3.97ppm. Six acetyl single peaks displayed clearly from 2.27ppm to 1.99ppm.

In the ^{13}C spectrum, seven signals appear in the carbonyl region at 170.36ppm, 170.32ppm, 170.06ppm, 169.64ppm, 169.36ppm, 168.18ppm and 157.67ppm. The first six carbonyl carbon signals were assigned to the acetyl groups, the last carbonyl carbon signal was assigned to 1-C. This carbonyl carbon signal confirmed the glucose ring was closed during the acetylation reaction. Two signals in the unsaturated carbon region at 137.37ppm and 131.59ppm were assigned to 2-C and 3-C. One signal in the anomeric region at 102.19ppm was assigned to 1'-C. Eight signals showed from 77.91ppm to 61.18ppm, represented the remaining carbons in the galactose and glucose rings. The last six signals from 20.84ppm to 20.20ppm were assigned to the methyl carbons of the acetyl groups.

Glumer et al.[70] also synthesised the same compound Monomer three **(58)**. They used D-glucono-lactone as the starting material, which they reacted in anhydrous acetic anhydride and triethylamine at 0°C. Then they used one equivalent of this sugar monomer to copolymerize with one equivalent of Sty, NVP, VAc respectively by free radical polymerization, using 2,2'-azoisobutyronitrile and dibenzoyl peroxide as initiators. The proton NMR spectra showed that the peaks of double bonds in the molecules all disappeared. Therefore it was decided to attempt this approach. The polymerizable acryloyl double bond is on the glucose. Hence polymerisation would be through the functionalised glucoses and the galactoses would remain pendant from the glucose backbone. In summary a polymer with pendant intact galactoses would result.

One equivalent of Monomer three **(58)** was co-polymerized with one equivalent of NVP in 2-methoxyethanol with "adzo88" as the initiator. The reaction was performed overnight. Next day a sample was taken to check proton NMR spectrum. The double bond peaks of Monomer three **(58)** still existed, but the double bonds of NVP had disappeared from the proton spectrum. These facts indicated that NVP had polymerised but Monomer three **(58)** had not polymerised with NVP.

As an alternative to NVP, *N*-isopropylacrylamide was used to copolymerize with Monomer three **(58)** using the same initiator and solvent but a longer reaction time was used. After two days a sample was checked by proton NMR. The result was the same as for NVP. The proton spectrum showed that *N*-isopropylacrylamide had polymerised but Monomer three **(58)** did not co-polymerise with it, nor was the homopolymer of **(58)** formed under these conditions.

These polymerisation conditions were the same as used for synthesising the polyamine but they did not work for Monomer three **(58)**. One reason for this might be that Monomer three **(58)** is a bulky molecule and the double bond is "hidden" in the glucose ring. This would make free radical attack leading to polymerisation harder to achieve.

2.5 Preparation of Synthetic Polymers

Polyamine (59)

The yields of pure Monomer one **(51)** and Monomer two **(57)** were usually very low after HPLC, thus amounts sufficient for polymerization studies were not obtained. However, crude monomers contained lactobionic acid **(45)** that directly affected the efficiency of polymerization, and usually gave acidic hydrogels, due to the existence of lactobionic acid **(45)**. The liver cells like to grow in a neutral environment, hence the acidic environment of an hydrogel will accelerate the death of cell at the surface. In order to overcome these disadvantages, we selected another way to make the lactosylated polymer. This idea came from Motherwell et al.[71] They designed "millipede" artificial enzymes. They used poly-allylamine for the backbone and

attached various combinations of carboxylic acids (some of which contained the well known active groups from the catalytic site of the enzymes) to form randomly functionalized polymers. Therefore instead of starting with the monomers, it was decided to make the polyamine **(59)** first and then graft the lactone **(46)** onto the polyamine backbone to achieve the lactosylated polymer. This approach would also allow, in addition to making similar polymers to the original target compounds, the possibility of grafting on many other small molecules.

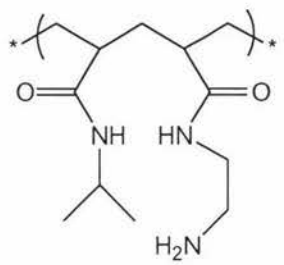

(59)

In this study firstly, *N*-acryloyl-*N*-Boc-ethylenediamine **(49)** was polymerized to achieve a polyamine backbone. One equivalent *N*-acryloyl-*N*-Boc-ethylenediamine **(49)** was co-polymerized with one equivalent *N*-isopropylacrylamide. "Azo88" was used as the initiator and the solvent was 2-methoxyethanol. The polymerization was performed overnight at 80°C. After the polymerization was completed, the proton NMR spectrum showed the peaks of the double bonds had disappeared, and other peaks in the molecule broadened. It was therefore concluded that polymerization had taken place and appeared to have gone to completion.

The polymer was dissolved in a 1:1 mixture of DCM:TFA to give the Boc-polyamine. The polyamine **(59)** was purified by dialysis with periodic water changes. The proton NMR spectra confirmed the formation of the polyamine **(59)**. One broad singlet signal at 3.86ppm was assigned to C**H**NH. The NHC$\mathbf{H}_2$ and C$\mathbf{H}_2$NH$_2$ displayed broad singlet as well at 3.67ppm and 3.09ppm respectively. The alkyl (-C$\mathbf{H}_2$-) polyamine backbone displayed from 2.30ppm to 1.30ppm, and the (C$\mathbf{H}_3$)$_2$ exhibited a broad singlet signal at 1.11ppm.

In the ^{13}C NMR spectrum, two signals in the carbonyl region displayed at 177.33ppm and 175.16ppm. One signal at 41.75ppm was assigned to NH**C**H. The CONH**C**H_2 and **C**H_2NH_2 displayed at 38.79ppm and 37.04ppm and the signal at 21.44ppm was assigned to the (**C**$H_3)_2$. However in carbon spectrum, carbon signals of CF_3COOH also appeared. The quartet from 163.28ppm to 162.22ppm was assigned to CF_3**C**OOH, and **C**F_3COOH displayed a quartet 120.68ppm to 111.97ppm. The conclusion is thus that the polyamine **(59)** was in its TFA salt form.

Lactosylated polyamine (60)

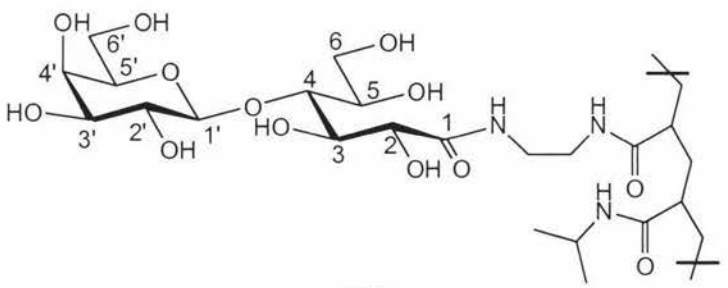

(60)

Having successfully synthesized polyamine **(59)**, the next step was to graft on the lactone **(46)** onto the polyamine **(59)**. The polyamine **(59)** TFA salt was dissolved in methanol, DIEA was added to remove TFA and release free amino groups. Finally lactone **(46)** was added to the solution. The reaction was carried out for 24hrs at room temperature. After the reaction was complete, the solvent was evaporated under reduced pressure. This lactosylated polyamine **(60)** was purified by dialysis with periodic water changes. After 24 hours, the solution was freeze-dried in vacuo. The proton NMR spectrum proved the structure of lactosylated polyamine **(60)**. In the spectrum all signals of lactone **(46)** became broader due to the formation of the lactosylated polymer **(60)**. 1'-H displayed a broad doublet at 4.53ppm, 2-H and 3-H exhibited broad singlet signal at 4.38ppm and 4.18ppm respectively. The remaining hydrogens of the lactone **(46)** and the NHC**H** showed multiple broad signals from 3.95ppm to 3.50ppm. The signals at 3.45ppm and 3.00ppm were assigned to (-NCH_2CH_2NH-). The signals from 2.28ppm to 1.38ppm were assigned to the alkyl backbone. The broad single peak at 1.10ppm was assigned to the (C**H**$_3)_2$.

Acryloyl polyamine (61)

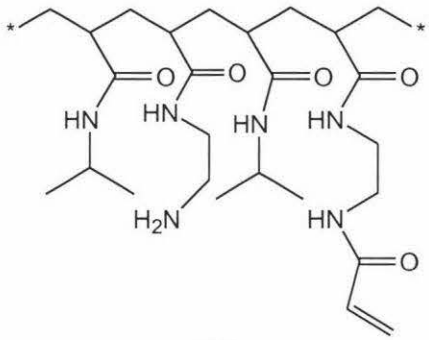

(61)

In order to produce a strong, viable hydrogel, the lactosylated polyamine **(60)** needs to be crosslinked. Therefore attachment of lactone **(46)** alone to the polyamine **(59)** backbone was not seen as sufficient. Grafting molecules that contained an active double bond was seen as a reasonable path to follow. Firstly, we used acryloyl chloride to introduce another neutral, strong amide bond into the polymer. Polyamine **(59)** and DIEA were dissolved in DMF, and acryloyl chloride in DMF solution was added dropwise. The solution was initially cooled in an ice-bath for two hours, and then reacted at room temperature for one day. The product was purified by dialysis with periodic water changes. Finally the solution was freeze-dried and a white polymer as a foam was obtained. The attachment of the acryloyl double bond containing moiety was proven by proton NMR. New peaks appeared at 6.22ppm and displayed broad multiple coupling pattern. These were assigned to the C**H**$_2$ of acryloyl double bond. Another new peak showed a broad doublet at 5.71ppm and was assigned to the C**H** of the acryloyl double bond. The other peaks displayed were the same as for the polyamine **(59)**. Therefore the desired acryloyl polyamine **(61)** had been synthesized. Next crosslinking of this material was attempted. The above acryloyl substituted polyamine **(61)** was dissolved in water, and treated with *N,N*'-methylene-bisacrylamide and ammonium peroxodisulphate. After degassing, TEMED was added and the hydrogel formed quickly.

Acryloyl lactosylated polyamine (62)

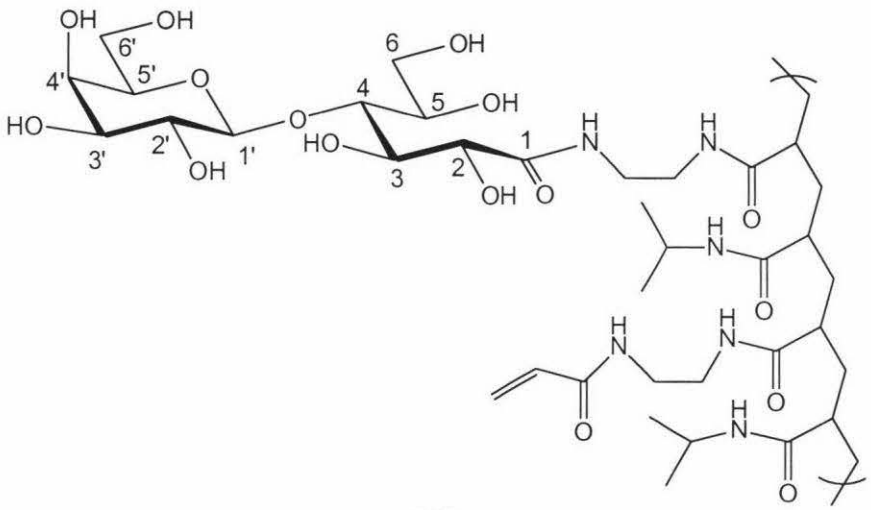

(62)

Since a hydrogel can be achieved from crosslinking the acryloyl polyamine **(61)**, next it was decided to the attach lactone **(46)** and acryloyl chloride together on the polyamine **(59)**. Firstly polyamine **(59)** and DIEA were dissolved in MeOH. The lactone **(46)** that was equivalent to half the amount of free amino groups on the polyamine **(59)** was added to the solution. The reaction was carried out overnight at room temperature. The reaction mixture was then purified by dialysis. This lactosylated polyamine **(60)** and DIEA dissolved in DMF and acryloyl chloride in DMF solution was added dropwise. Initially this reaction proceeded in an ice-bath and then was left to react at room temperature for 2 days. The solution was dialyzed against water (changed 8 times a day) for 2 days, and finally freeze-dried in vacuo. The structure of this lactosylated acryloyl polymer **(62)** was confirmed by proton NMR spectrum. All characteristic signals of acryloyl double bond and lactose were displayed at the correct positions in the spectrum. Therefore the desired acryloyl "lactosylated" polyamine **(62)** had been synthesized. This disubstituted polyamine **(62)** was dissolved in water, and treated with *N,N'*-methylene-bisacrylamide and ammonium peroxodisulphate. After degassing, TEMED was added. However, unlike the acryloyl polyamine **(61)**, this acryloyl "lactosylated" polyamine **(62)** did not form a gel. The reasons for this are probably because the crosslinker was too short compared with the big lactose, and could not crosslink the two chains, therefore no gel formed.

Chapter 3: Conclusion and Future studies

3.1 Conclusion

In this study, three monomers were synthesized as the first stage in preparing polymers suitable as supports for hepatocyte growth. The monomers maintained the geometry of galactose in order to promote the adhesion, proliferation and viability of hepatocytes *in vitro*; two of them had a polymerizable double bond linked with lactose through amide bond at glucose residue and one contained the double bond in the glucose ring.

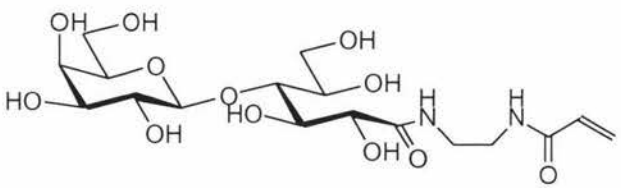

Figure 3.1. Monomer one **(51)**

The attempted polymerization of Monomer one **(51)** was hindered by the presence of lactobionic acid **(45)**, so that Monomer one **(51)** did not readily form a hydrogel. Although pure monomer could be isolated through HPLC, the yield was unsatisfactory. Therefore an alternative strategy was selected. Polyamine **(59)** was the core of this strategy. Because many free amino groups hung from the alkyl backbone, different pendant groups could be attached to the polymer backbone through amide bonds. One example was lactone **(46)** and the lactosylated polyamine **(60)** could be easily purified by dialysis to get rid of lactobionic acid **(45)**. Fully lactosylated polyamine **(60)** and partially lactosylated polyamine **(60)** could be obtained by varying amount of lactone **(46).** Partially lactosylated polyamine **(60)** still contained free amino groups in the backbone, therefore glutaraldehyde was used to crosslink two free amino groups in different chains to give the crosslinked lactosylated polyamine. The crosslinked polyamine also obtained by using glutaraldehyde as crosslinker. This crosslinked lactosylated polyamine was cast as thin films for use in cell trials.

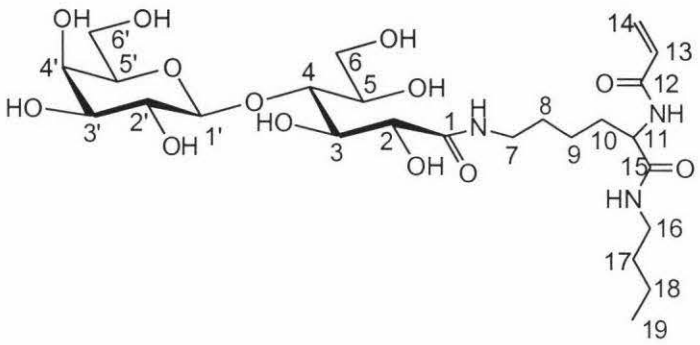

Figure 3.2. Monomer two **(57)**

Monomer two **(57)** was another option. It not only contained lactose but also contained lysine **(52)**. A natural amino acid as part of the polymer or hydrogel will always be of interest in tissue engineering. However Monomer two has not been polymerized or been submitted for any biological tests due to time constraints, but has only been characterized by NMR and MS. Monomer two still faced the same problem as Monomer one (the presence of lactobionic acid **(45)** in the preparation, and low recovery following HPLC purification). Therefore a graft polymer approach, as adopted for Monomer one, is probably the better choice for future work.

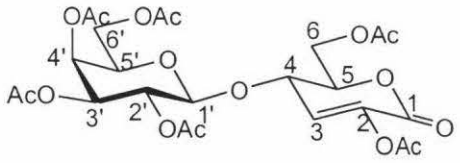

Figure 3.3. Monomer three **(58)**

Monomer three **(58)** had an activated double bond in the glucose ring, so in principle did not need any extra polymerizable double bond attached to it. However this double bond was not as reactive as desired, probably for steric reasons. The copolymerization with NVP and *N*-isopropylacryl amide did not succeed.

In a conclusion, three monomers were successfully synthesized and characterized. The desired polymer scaffold-crosslinked lactosylate polyamine was also made, and found to perform well in initial cell trials.

3.2 Future studies

The lactosylated polyamine **(60)** will be employed in full cell trials with several cell types, such as rat hepatocytes, nerve cells and stem cells. This is important because different cells have different affinities for different materials.

Natural extensions to the current work include the preparation of polymers based on Monomer two **(57)** and on other related carbohydrate-amino acid conjugates, and the preparation of further derivatives of polyamine **(59)**, dependant of course on the kind of cells required to interact with the polymer or hydrogel. Similar polymers incorporating glucose instead of lactose must be prepared, in order to prove that the galactose residue makes a difference. This might be simply accomplished through the chemical cleavage of the galactose residue off the lactosylated polymer.

The incorporation of RGD sequences into the polymers, and the use of different crosslinking groups, should be investigated, in order to produce polymers with different or improved cell affinities. Where new materials have performed well as thin films, the preparation of three-dimensional sponge-like networks is desirable.

Chapter 4: Materials, Methods and Experimental

4.1 Materials

Lactose, ammonium persulfate, N-butylamine, 8-hydroxyquinoline, hydrochloric acid, acetic acid, Amberlite IR-120 (H^+), fuchsin (4-rosaline hydrochloride) were purchased from BDH Chemicals Ltd Poole England. Di-t-butyl dicarbonate was from Auspep Pty. Ltd. Australia. 1-Ethyl-3-(3-dimethylaminopropyl)-carbodiimide hydrochloride and N-hydroxysuccinimide were from Acros Organics New Jersey USA. Ethylenediamine came from Lancaster, England. Trifluoroacetic acid was peptide synthesis grade and was obtained from Applied Biosystems. 1,1'-Azobis-(cyclohexanecarbonitrile) and N-isopropylacrylamide were purchased from Aldrich Chemical Company, Inc. USA. Glutaraldehyde and N,N,N',N'-tetramethyl-ethylenediamine (TEMED) from Sigma Chemical Co. USA. Sodium borohydride and N-N-di-iso-propylethylamine (DIEA) were obtained from Riedel-de Haen, Germany. Potassium hydroxide, lysine.HCl, and $CuSO_4.5H_2O$ were from Merck Germany. Iodine was from AJAX Chemicals, Australia. Magnesium sulfate anhydrous (extra pure), sodium hydrogen carbonate, sodium hydroxide and sodium bisulfite were from Scharlau Chemie, Spain. Periodic acid was supplied from Scientific Supplies Ltd Auckland. Methanol, diethyl ether, DCM, 2-methoxyethanol, acetonitrile, 2-methylpropan-2-ol, pyridine, acetic anhydride, hexane, ethyl acetate, DMF were analytical grade. Milli-Q water was used throughout this study unless stated otherwise.

4.2 Methods

4.2.1 Method for estimating free amino groups in the polyamine and lactosylated polyamine products.

4.2.1.1 Polyamine

Polymerization was started with equal amounts of *N*-iso-propylacrylamide and *N*-Boc-*N'*-acryloylethylenediamine. After the copolymer had been deprotected and dialyzed, NMR was employed to prove the structure of the copolymer. The proton integrals from NMR spectrum indicated the ratio of these two compounds in the

copolymer was approximately 1:1. Therefore the unit molecular weight in this copolymer was 227g/mol.

4.2.1.2 Lactosylated polyamine

After the lactosylated polyamine had been dialyzed, proton integrals from the NMR spectrum were used to obtain the percentage of lactone. As the polyamine's free amino group value had been determined as approximately 1:1 with isopropyl group, the number of free amino groups left after lactosylation can be estimated.

4.2.2 Measurement of the molecular weight of polyamine and lactosylated polyamine by FPLC

FPLC conditions:

Mobile phase: 0.05M Na/K phosphate buffer containing 0.15M NaCl, pH 7.0

Mw standards: (1) phosphorylase b---Mw=97,400

(2) BSA---Mw=67,000

(3) albumin, egg---Mw=45,000

(4) trypsinogen---Mw=24,000

(5) alpha-lactalbumin---Mw=14,200

Void volume determination: Blue Dextran 2000

FPLC---Flow rate: 0.5ml/min

Injection volume: 50µl

Chart speed: 0.2cm/min

UV detection: 214nm

Polyamine concentration: 5mg/ml

Lactosylated polyamine concentration: 5mg/ml

4.2.3 Qualitative measurement of lactose

The colorimetric assay used for measuring polysaccharides was based on the periodic acid/Schiff's stain method. This method describes an easy and sensitive colorimetric method for measuring polysaccharides that are oxidized by periodate. This method is divided into two parts: firstly, preparation of the Schiff's reagent, and secondly, the coupling of the oxidized polysaccharides to the Schiff's base. Schiff's reagent is prepared by dissolving 0.05g of pure Fuchsin (4-rosaline hydrochloride) in 50ml of

distilled water, adding 2ml of saturated sodium bisulfite solution. This solution, after sitting for 1 hr was treated with 1ml of concentrated hydrochloric acid and allowed to stand overnight. This reagent is practically colorless and very sensitive. Periodate solution was prepared by adding 10μl of 50% periodic acid to 10ml of 7% acetic acid solution. The concentrations of polyamine and lactosylated polyamine were 50μg/ml.

The test was carried out as follows: 0.1ml periodate solution was added to 1ml sample solution and the mixture placed in a water-bath at 37°C for two hours. Then 0.1ml Schiff's reagent was added and held in the water-bath at 37°C for 30mins. A positive result is the formation of a violet-purple solution.

4.2.4 General experimental methods

Nuclear magnetic resonance spectra were recorded on Bruker 400 Ultrashield TM and Bruker 500 Ultrashield TM, as indicated. Samples were prepared as D_2O and $CDCl_3$ solutions in 5mm sample tubes. Proton spectra were referenced to the residual H_2O and $CHCl_3$ signal at 4.78ppm and 7.28ppm. The subscripts A and B are used to distinguish between the upfield and downfield signals of an ABX system.

Mass spectra were recorded on a Micromass ZMD single quadrupole electrospray mass spectrometer. Samples were ionized by electron spray.

IR spectra were recorded on NICOLET 5700 FT-IR. Samples were prepared as KBr discs.

Reverse phase HPLC was performed on a Shimadzu system: Shimadzu Liquid Chromatograph LC-6A with a SCL-6A controller. The following refer to the separation details used: solvent A: 98% water, 2% acetonitrile, 0.1% TFA, solvent B: 10% water, 90% acetonitrile, 0.1% TFA, gradient 0% B -> 20% B over 45min.

Thin-layer chromatography was preformed with silica gel (Silica 60 A C. C 40-63μm), developed in the solvent system indicated.

4.3 Experimental

4.3.1 Synthesis of lactone **(46)**

4.3.1.1 Potassium lactonate ***(44)***

Iodine (8.53g, 80.5mmol) was dissolved in methanol (120ml) at 40°C and added to lactose (6.01g, 17.6mmol) in warm water (25ml) at 45°C. A 4% potassium hydroxide solution in methanol (200ml) also at 45°C was then added dropwise with stirring until the colour of iodine disappeared. The solution was then cooled in an ice-bath. The precipitated crystalline product was filtered, washed with ice-cold methanol and then ice-cold ether. The crude product was obtained as a white solid (10g). The crude product was dissolved in water and recrystallized from methanol at 40°C to yield white crystals, 5.30g (79 %) of potassium lactonate **(44).**

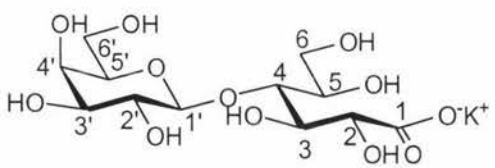

(44)

NMR δ (500Hz, D_2O) 4.54ppm (1H, *d J*=7.8Hz, 1'-H), 4.16ppm (1H, *d J*=3.0Hz, 2-H), 4.09ppm (1H, *dd J*=5.3Hz *J*=3.0Hz, 3-H), 3.98ppm (1H, *tri J*=5.3Hz, 4-H), 3.96ppm (1H, *m*, 5-H), 3.90ppm (1H, *br d J*=3.4Hz, 4'-H), 3.85ppm (2H, *dd J*=3.3Hz *J*=12.1Hz, 6-H), 3.83-3.68ppm (2H, *m*, 5'-H 6'-H), 3.66ppm (1H, *dd J*=10.0Hz *J*=3.5Hz, 3'-H), 3.57ppm (1H, *dd J*=10Hz *J*=7.8Hz, 2'-H)

NMR ^{13}C (500Hz, D_2O) 178.5ppm (1-C), 103.5ppm (1'-C), 81.7ppm (4-C), 75.4ppm (5'-C), 72,6ppm, 72.4ppm, 72.3ppm, 71.8ppm, 71.6ppm, 71.2ppm (2'-C, 3'-C, 2-C, 3-C, 5-C), 68.7ppm (4'-C), 61.9ppm, 61.1ppm (6'-C, 6-C)

ES (-) Mass spectrum

Mw=396.38g/mol

Parent ion ($M\text{-}K^+$) =357.14

IR (KBr)

ν_{O-H}3389.3cm^{-1}, ν_{C-H} 2934.9cm^{-1}, 2903.9cm^{-1}, $\nu_{C=O}$1604.4cm^{-1}.

4.3.1.2 Lactobionic (acid) lactone (46)

Potassium lactonate **(44)** (5.30g) was converted to the free acid by stirring the aqueous solution (20ml) with 10g of 'Amberlite' resin IR-120 (H^+) for 10min. The solution was filtered and the filtrate freeze-dried *in vacuo.* The product, lactobionic acid **(45)** was obtained as an impure white solid 4.59g (92 %).

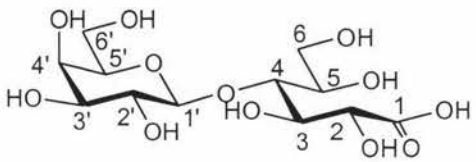

(45)

NMR δ (400Hz, D_2O) inter alia 4.49ppm (1H, *d* *J*=7.1Hz, 1'-H), 4.48ppm (1H, *d* *J*=2.9Hz, 2-H), 4.16ppm (1H, *dd* *J*=4.5Hz *J*=3.2Hz, 3-H), 4.0-3.5ppm (10H, m, 4-H, 5-H, 6-H, 2'-H, 3'-H, 4'-H, 5'-H, and 6'-H)

IR (KBr)

ν_{O-H} 3420.3cm^{-1}, $\nu_{C=O}$ 1729.7cm^{-1}.

Lactobionic acid **(45)** (4.59g, 12.8mmol) was dissolved in 2-methoxyethanol (100ml). The solution was distilled at 120°C until most of the solvent was removed; the remaining solvent was evaporated under reduced pressure and the residue dried *in vacuo* to yield a white solid, impure lactobionic acid lactone **(46)** in 4.01g yield (92 %).

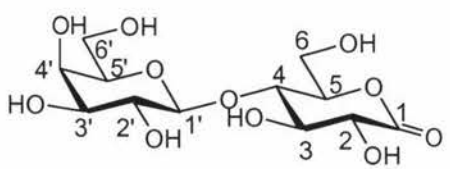

(46)

NMR δ (400Hz, D_2O) inter alia 4.45ppm (1H, *d* *J*=7.8Hz, 1'-H), 4.36ppm (1H, *ddd*

J=9.0Hz *J*=3.3Hz *J*=2.6Hz, 5-H), 4.21ppm (1H, *d J*=10.2Hz, H-2), 4.09ppm (1H, *tri J*=9.1Hz, 3-H), 4.0-3.5ppm (9H, m, 4-H, 6-H, 2'-H, 3'-H, 4'-H, 5'-H, and 6'-H)

IR (KBr)

ν_{O-H} 3413.1cm^{-1}, $\nu_{C=O}$ 1733.0cm^{-1}.

4.3.2 Synthesis of Monomer one **(51)**

4.3.2.1 Mono-Boc-ethylene diamine ***(48)***

Ethylene diamine (1.00ml, 15.0mmol) was dissolved in 10ml DCM. A solution of di-tert-butyldicarbonate (436mg, 2.00mmol) in 10ml DCM was added dropwise with stirring. The mixture was stirred for 1 hour with cooling in a water bath at ambient temperature. The solvent was evaporated under reduced pressure. The residue was dried *in vacuo*. Colorless oil was obtained and used without further purification (440mg).

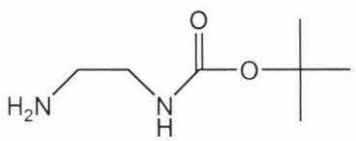

(48)

NMR δ (400Hz, $CDCl_3$) 5.15ppm (1H, *br* s, N**H**); 3.11ppm (2H, *br d J*=5.67Hz, C$\mathbf{H}_2$NH); 2.74ppm (2H, *t J*=5.9Hz, $H_2NC\mathbf{H}_2$); 1.39ppm (9H, *s*, t-Bu).

IR (KBr)

ν_{N-H} 3357.5cm^{-1}, ν_{C-H}2976.9 cm^{-1} and 2932.5 cm^{-1}, $\nu_{C=O}$1692.8 cm^{-1}.

ES (+) Mass spectrum

Mw=160.22g/mol

Parent ion (M+1) =160.96

4.3.2.2 N-Boc-N'-acryloylethylene diamine ***(49)***

The crude *N*-Boc-ethylene diamine **(48)** (440mg) was dissolved in 15ml DCM and the solution cooled in an ice-bath. DIEA (514µl, 3.00mmol) was added, followed by acryloyl chloride (162µl, 2mmol). The mixture was warmed to room temperature and stirred under a drying tube for 3 hours. The colorless solution was washed with 0.1M HCl twice, the organic phase dried with $MgSO_4$, and the solvent was evaporated under reduced pressure. The residue was dried *in vacuo*. *N*-Boc-*N*'-acryloyl-ethylene diamine **(49)** was obtained as a white solid, 350mg (1.64mmol, 82%). The white solid was purified on a silica column with a mobile phase gradient from 50%: 50% ethyl acetate:hexane to 100% ethyl acetate. The final product was a white solid, 200mg (0.93mmol, 57%).

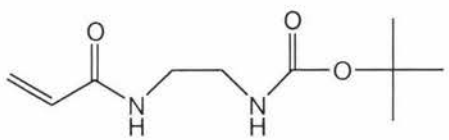

(49)

NMR δ (500Hz, $CDCl_3$) 6.59ppm (1H, *br s*, OCN**H**), 6.2ppm (2H, *m*, C**H**$_2$=CH), 5.65ppm (1H, *dd J*=10.3Hz *J*=1.2Hz, CH_2=C**H**), 5.07ppm (1H, *br s*, **H**NCOO), 3.45ppm (2H, *dd J*=5.3Hz *J*=11Hz, OCHNC**H**$_2$), 3.33ppm (2H, br *t J*=5.5Hz, **H**$_2$CNHCOO), 1.44ppm (9H, *s*, t-Bu**).**

ES (+) Mass spectrum

Mw=214.26g/mol

Parent ion (M+1) =214.89

TLC (Ethyl acetate) R_f=0.448

IR (KBr)

ν_{N-H} 3301.6 cm^{-1}), ν_{C-H} 3076.7 cm^{-1}, ν_{C-H} 2978.6 cm^{-1} and 2932.2 cm^{-1}, $\nu_{C=O}$ 1696.0 cm^{-1}, $\nu_{C=O}$ 1662.8 cm^{-1}, $\nu_{C=C}$ 1628.9 cm^{-1}.

4.3.2.3 N-Acryloyl-ethylene diamine ***(50)***

N-Boc-*N'*-acryloylethylene diamine **(49)** (350mg, 1.64mmol) was dissolved in 20ml of a 50:50 mixture of trifluoroacetic acid and DCM, and the solution stirred for 30min. The solvent was removed under reduced pressure and dried *in vacuo*, giving *N*-acryloylethylene diamine **(50)** with TFA salt as a white oil 340.7mg (1.50mmol, 91 %).

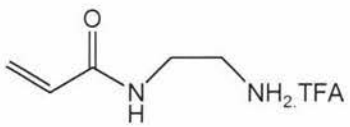

(50)

NMR δ (500Hz, MeOH) 6.24ppm (2H, *m*, C**H**$_2$=CH); 5.78ppm (1H, *dd J*=9.55Hz *J*=1.85Hz, CH$_2$=C**H**); 3.57ppm (2H, *t J*=5.85Hz, HNC**H**$_2$); 3.17ppm (2H, *t J*=5.78Hz, C**H**$_2$NH$_2$).

ES (+) Mass spectrum

Mw=114.15g/mol

Parent ion (M+1) =114.92

IR

ν_{N-H} 3276.6 cm^{-1}, ν_{C-H} 3075.9 cm^{-1}, ν_{C-H} 2933.5 cm^{-1}, $\nu_{C=O}$ 1667.3 cm^{-1}, $\nu_{C=O}$ 1628.9 cm^{-1}.

4.3.2.4 Monomer 1 ***(51)*** *– from the reaction of N-acryloylethylene diamine* ***(50)*** *with lactobionic acid lactone* ***(46)***

N-Acryloyl-ethylene diamine **(50)** TFA salt (340.7mg, 1.50mmol) was dissolved in 20ml MeOH. DIEA (0.50ml, 3.00mmol) and the lactone **(46)** (510mg, 1.50mmol) were added, and the solution stirred at room temperature under a drying tube overnight. The solution was evaporated to dryness *in vacuo.* The residue was dissolved in 20ml water, mixed with 'Amberlite' resin IR-120 (H^+) resin (10g) for 30min to remove DIEA. The resin was removed by filtration and the filtrate was then

freeze-dried. The monomer one **(51)** was obtained as a white solid (470mg). The monomer one **(51)** was purified by reverse phase HPLC (310mg).

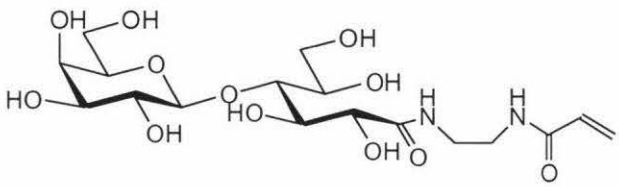

(51)

NMR δ (500Hz, D_2O) 6.24ppm (2H, *m*, C**H**$_2$=CH), 5.77ppm (1H, *dd J*=9.95Hz *J*=01.4Hz, CH_2=C**H**), 4.46ppm (1H, *d J*=7.85Hz, 1'-H), 4.31ppm (1H, *d J*=2.7Hz, 2-H), 4.09ppm (1H, *tri J*=3.38Hz, 3-H), 3.89ppm (1H, *tri J*=5.37Hz, 4-H), 3.85ppm (1H, *m*, 5-H), 3.83ppm (1H, *d J*=3.15Hz, 4'-H), 3.78ppm (2H, *dd J*=12Hz J=3.2Hz, 6-H), 3.73—3.62ppm (3H, *m*, 5'-H 6'-H), 3.58ppm (1H, *dd J*=10Hz *J*=3.35Hz, 3'-H), 3.49ppm (1H, *m*, 2'-H), 3.35ppm (4H, *br tri* J=3.8Hz, HNC**H**$_2$C**H**$_2$NH)

NMR ^{13}C (500Hz, D_2O) 174.6ppm, 168.8ppm (**C**=O), 129.9ppm (CH_2=**C**H), 127.4ppm (**C**H_2=CH), 103.4ppm (1'-C), 80.9ppm (4-C), 75.3ppm (5'-C), 72.4ppm, 72.3ppm, 71.4ppm, 71.0ppm, 70.4ppm (2'-C, 3'-C, 2-C, 3-C, 5-C), 68.6ppm (4'-C), 61.9ppm, 61.0ppm (6'-C, 6-C), 38.6ppm, 38.4ppm (HN**C**H_2**C**H_2NH)

ES (+) Mass spectrum

Mw=454.43g/mol

Parent ion (M+1) =455.10

IR (KBr)

$\nu_{O\text{-}H,N\text{-}H}$ 3377.8cm^{-1}, $\nu_{C=O}$ 1657.4cm^{-1}.

4.3.3 Synthesis of Monomer two ***(57)***

4.3.3.1 N^{ε}-Boc-lysine ***(53)***

Lysine.HCl (1g, 5.48mmol) was dissolved in 10ml of aqueous 2M $NaHCO_3$, 10ml aqueous $CuSO_4.5H_2O$ (0.685g, 2.74mmol) and another $NaHCO_3$ (0.46g) was added, and then a solution of di-tert-butyldicarbonate (1.62g, 7.43mmol) in 7ml acetone was added. The mixture was stirred for 24hr at room temperature. MeOH (6ml) was added into the solution, stirred for another 24hr. Water (10ml) and ethyl acetate (10ml) were added, the mixture was stirred evenly and filtered. The blue solid was obtained (3.08g). The blue solid (3.08g) was dissolved in 120ml water and 8-hydroxyquinoline (2.1mg, 14.43mmol) was added, the mixture was stirred for 5hr at room temperature. The mixture was filtered, the white solid was dissolved in another 60ml water and stirred for a day. The solution was filtered again, and the aqueous was washed with ethyl acetate (2*100ml). The aqueous phase was frozen and dried *in vacuo*. White solid was obtained, 1.043g (4.24mmol, 77.4%).

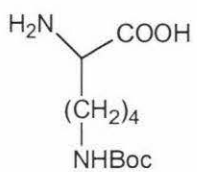

(53)

NMR δ (500Hz, D_2O) 3.70ppm (1H, *tri J*=6.13Hz, C**H**), 3.07ppm (2H, *tri J*=6.68Hz, C$\mathbf{H}_2$NHCO), 1.85ppm (2H, *m*, CHC$\mathbf{H}_2$), 1.53ppm (2H, *m*, C$\mathbf{H}_2$CH_2NHCO), 1.43ppm (9H, *s*, t-Bu), 1.39ppm (2H, *m*, CHCH_2C$\mathbf{H}_2$).

ES (+) and ES (-) Mass spectrum
Mw=246.30g/mol
Parent ion (M+1) =247.12
Parent ion (M-1) =245.08

4.3.3.2 N^{α}–Acryloyl-N-Boc-butylamide-L-lysine ***(55)***

Lys(Boc) **(53)** (1.00g. 4.07mmol) was dissolved in a mixture of 10ml of aqueous 1M NaOH and 10ml CH_3CN. Acryloyl chloride (396µl, 4.88mmol) was added dropwise to the solution. The mixture was stirred at room temperature under a drying-tube for two hours. The solution was acidified to pH 1 with 1M HCl, and extracted with ethyl

acetate (3x10ml). The ethyl acetate phases were combined and dried with $MgSO_4$. The solvent was evaporated under reduced pressure. The residues were dried *in vacuo*, and white solid N^{α}-Acryloyl-N^{ε}-Boc-L-lysine **(54)** was obtained (1.09g, 3.62mmol). Yield was 89 %.

The crude white solid **(54)** (1.09g, 3.62mmol) was dissolved in 10ml DCM, N-hydroxysuccinimide (458.3mg, 3.98mmol) and EDC.HCl (763.4mg, 3.98mmol) were added. The solution was stirred at room temperature under a drying-tube for 2hrs. Then *n*-butylamine (400µl, 3.98mmol) was added to the solution directly, stirred at room temperature under a drying-tube over night. The solvent was evaporated to dryness under reduced pressure. A white solid was obtained (0.83g, 2.33mmol). Yield was 64 %. The white solid was purified by silica gel chromatography; the mobile phase was hexane and ethyl acetate. The product was a white solid, 0.33g (40%).

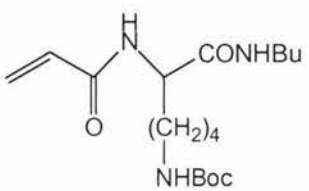

(55)

NMR δ (500Hz, $CDCl_3$) 6.25ppm (2H, *m*, C**H**$_2$=CH), 5.67ppm (1H, *dd J*=10.05Hz *J*=1.55Hz, CH_2=C**H**), 4.55ppm (1H, *dd J*=14.05Hz *J*=7.8Hz, C**H**), 3.21ppm (2H, *m*, CHCONHC**H**$_2$), 3.09ppm (2H, *m*, C**H**$_2$NHBoc), 1.85ppm (2H, *m*, CHC**H**$_2$), 1.56-1.26ppm (8H, *m*, $CHCH_2C\mathbf{H}_2C\mathbf{H}_2$, $C\mathbf{H}_2C\mathbf{H}_2CH_3$), 1.44ppm (9H, *s*, t-Bu), 0.92ppm (3H, *tri J*=7.3Hz, C**H**$_3$).

NMR ^{13}C (500Hz, D_2O) 172.2ppm, 165.8ppm, 156.1ppm (C=O), 130.7ppm (CH_2=**C**H), 126.5ppm (**C**H_2=CH), 78.9ppm (**C**-$(CH_3)_3$), 53.1ppm (HN**C**HCO), 40.1ppm (**C**H_2NHBoc), 39.2ppm (CHCONH**C**H_2), 32.2ppm (CH**C**H_2), 28.4ppm (C-(**C**$H_3)_3$), 13.7ppm (CH_2**C**H_3), 31.3ppm, 29.4ppm,22.7ppm, 19.9ppm ($CHCH_2\mathbf{C}H_2\mathbf{C}H_2$, $\mathbf{C}H_2\mathbf{C}H_2CH_3$).

IR (KBr)

ν_{N-H} 3287cm^{-1}, ν_{C-H} 3055.7cm^{-1}, ν_{C-H} 2960.8cm^{-1} and 2933.9cm^{-1}, $\nu_{C=O}$ 1693.3cm^{-1}, $\nu_{C=O}$ 1650.2cm^{-1}, $\nu_{C=C}$ 1624.9cm^{-1}.

TLC (ethyl acetate) R_f=0.48

ES (+) Mass Spectrum
Mw=355.47g/mol
Parent ion (M+1) =356.13

4.3.3.3 N^{α}–Acryloyl-n-butylamide-L-lysine ***(56)***

N^{α}–Acryloyl-*N*-Boc-butylamide-L-lysine **(55)** (330mg) was dissolved in a mixture of 10ml DCM and 10ml CF_3COOH, stirred at room temperature for 30min. The solvent was evaporated under reduced pressure and dried *in vacuo.*

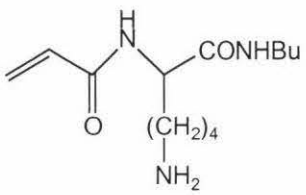

(56)

NMR δ (500Hz, D_2O) 6.30ppm (2H, *m*, C**H**$_2$=CH); 5.80ppm (1H, *dd J*=10.15Hz *J*=1.2Hz, CH_2=C**H**); 4.29ppm (1H, *dd J*=8.65Hz *J*=5.8Hz, C**H**); 3.21ppm (2H, *m*, CONHC**H**$_2$), 3.00ppm (2H, *tri J*=7.35Hz, NH_2C**H**$_2$); 1.87-1.66ppm (4H, *m*, CHCH2, NH_2CH_2C**H**$_2$); 1.49-1.41ppm (4H, *m*, $CHCH_2$C**H**$_2$, $CONHCH_2$C**H**$_2$), 1.29ppm (2H, *m*, C**H**$_2CH_3$), 0.87ppm (3H, *tri J*=7.38Hz, C**H**$_3$)

NMR ^{13}C (500Hz, D_2O) 173.63ppm 168.47ppm (C=O), 129.22ppm (CH_2=**C**H), 128.26ppm (**C**H_2=CH), 54.01ppm (**C**H), 39.15ppm 39.05ppm (CONH**C**H_2, NH_2**C**H_2), 30.51ppm 30.40ppm ($CHCH_2$**C**H_2, $CONHCH_2$**C**H_2), 26.24ppm 22.13ppm (CH**C**H_2, NH_2CH_2**C**H_2), 19.29ppm (**C**H_2CH_3), 12.91ppm (**C**H_3)

ES (+) Mass spectrum
Mw=255.36g/mol
Parent ion (M+1) =256.10

4.3.3.4 Monomer 2 ***(57)*** *– from the reaction of N^{α}-acryloyl-butylamide-L-lysine* ***(56)*** *with lactobionic acid* ***(45)*** *lactone* ***(46)***

N^{α}–Acryloyl-butylamide-L-lysine **(56)** (482mg) was dissolved in 20ml MeOH, DIEA (0.32ml, 1.89mmol) was added, followed by the mixture of lactobionic acid **(45)** lactone **(46)** (428.4mg, 1.26mmol). The mixture was stirred at room temperature under a drying-tube overnight. The solution was evaporated under reduced pressure and dried *in vacuo.* Impure monomer two **(57)** (200mg) was purified by reverse phase HPLC. The final product was obtained as a white solid (140mg).

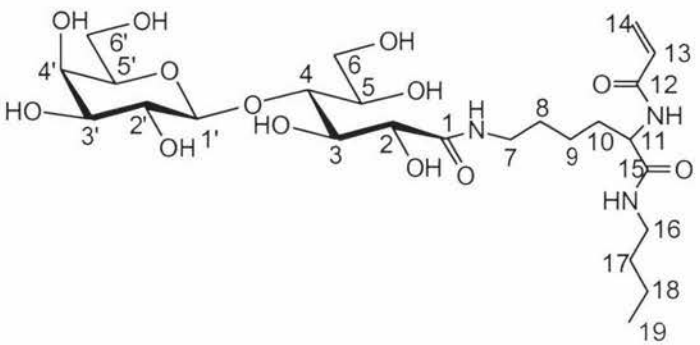

(57)

NMR δ (400Hz, D_2O) 6.2ppm (2H, *m*, 14-H), 5.7ppm (1H, *dd J*=10.1Hz *J*=1.5Hz, 13-H), 4.5ppm (1H, *d J*=7.7Hz, 1'-H), 4.3ppm (1H, *d J*=2.76Hz, 2-H), 4.2ppm (1H, *dd J*=8.44Hz *J*=5.8Hz,11-H), 4.1ppm (1H, *t J*=3.34Hz, 3-H), 3.92ppm (1H, *tri J*=5.4Hz, 4-H), 3.88ppm (1H, *m*, 5-H), 3.86ppm (1H, *d J*=3.26Hz, 4'-H), 3.82ppm (2H, *dd J*=11.9Hz *J*=3.2Hz, 6-H), 3.74—3.70ppm (3H, *m*, 5'-H, 6'-H), 3.62ppm (1H, *dd J*=10Hz *J*=3.4Hz, 3-H), 3.51ppm (1H, *dd J*=9.9Hz *J*=7.7Hz, 2-H), 3.20ppm (2H, *tri J*=6.87Hz, 7-H), 3.14ppm (2H, *m*, 16-H), 1.73ppm (2H,*m*, 10-H), 1.50ppm (2H, *m*, 8-H), 1.42ppm (2H, *m*, 17-H), 1.34ppm (2H, *m*, 9-H), 1.27ppm (2H, *m*, 18-H), 0.82ppm (3H, *tri J*=7.35Hz, 19-H)

NMR ^{13}C (400Hz, D_2O) 174.6ppm, 174.4ppm, 169.0ppm (C=O), 129.1ppm (13-C), 128.0ppm (14-C), 104.3ppm (1'-C), 81.3ppm (4-C), 75.6ppm (5'-C), 72.74ppm, 72.72ppm, 71.7ppm, 71.3ppm, 70.7ppm (2-C, 3-C, 2'-C, 3'-C, 5-C), 68.9ppm (4'-C), 62.5ppm and 61,6ppm (6-C, 6'-C), 54.6ppm (11-C), 39.6ppm and 39.3ppm (7-C, 16-

C), 31.2ppm and 31.0ppm (10-C, 8-C), 28.6ppm (17-C), 23.0ppm (9-C), 18.9ppm (18-C), 13.2ppm (19-C)

ES (-) Mass spectrum

Mw=595.42g/mol

Parent ion (M-1) =594.26

TLC (Ethyl acetate/MeOH/H_2O=85/30/10 v/v) R_f=0.48

4.3.4 Synthesis of Monomer three **(58)**

Potassium lactobionic acid **(44)** (1.00g, 2.65mmol) was dissolved in 7ml ice-cold pyridine, acetic anhydride (7ml) was added and the solution stirred for four days. The solution was poured into ice-cold saturated aqueous sodium chloride solution, and a gummy material came out of solution. The mixture was filtered, the gummy lumps were collected then dissolved into DCM and dried over magnesium sulfate. The organic solution was evaporated under reduced pressure. The residues were dried *in vacuo*. The silica column was used to purify the compound; the mobile phase was hexane and ethyl acetate. The product was obtained as a white solid 800mg (1.59mmol, 60.1 %).

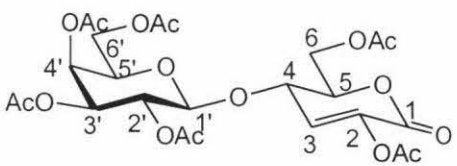

(58)

NMR δ (400Hz, $CDCl_3$) 6.68ppm (1H, *d J*=2.33Hz, 3-H), 5.40ppm (1H, *d J*=2.6Hz, 4'-H), 5.23ppm (1H, *dd J*=10.4ppm *J*=7.93ppm, 2'-H), 5.03ppm (1H, *dd J*=10.4Hz *J*=3.4Hz, 3'-H), 4.70ppm (1H, *dd J*=9.4Hz J-2.3Hz, 4-H), 4.65ppm (1H, *d J*=7.98Hz, 1'-H), 4.62ppm (1H, *m*, 5-H), 4.36ppm (1H, *dd J*=12.48Hz *J*=2.49Hz, 6-H_A), 4.26ppm-4.13ppm (2H, *m*, 6-H_B 6'-H_B), 4.12ppm (1H, *dd J*=11.35Hz *J*=6.24Hz, 6'-H_A), 3.97ppm (1H, *tri J*=6.58ppm, 5'-H), 2.27ppm 2.18ppm 2.15ppm 2.09ppm 2.07ppm 1.99ppm (18H, *s*, OC**H**$_3$)

NMR ^{13}C (400Hz, $CDCl_3$) 170.36ppm 170.32ppm 170.06ppm 169.94ppm 169.36ppm 168.18ppm (**C**OCH_3), 157.67ppm (1-C), 137.37ppm 131.59ppm (2-C 3-C), 102.19ppm (1'-C), 77.91ppm 71.04ppm 70.43ppm 69.90ppm 68.37ppm 66.71ppm 61.47ppm 61.18ppm (4-C, 5-C, 6-C, 2'-C, 3'-C, 4'-C, 5'-C, 6'-C), 20.84ppm 20.60ppm 20.52ppm 20.49ppm 20.41ppm 20.20ppm (CO**C**H_3)

4..3.5 Synthetic Polymer

4.3.5.1 Polymerization of N-acryloylethylene diamine lactone (Monomer 1) ***(51)***

The Monomer one **(51)** (681mg, 1.50mmol) and *N*-isopropylacrylamide (168mg, 1.50mmol) were dissolved in 10ml water and the solution was deoxygenated by bubbling N_2 for 30mins. Ammonium persulfate (60mg) and TEMED (570mM/L, 2.6ml) were added, and the mixture stirred at room temperature for 24hr. The solution was dialyzed for two days against water with 8 changes per day.

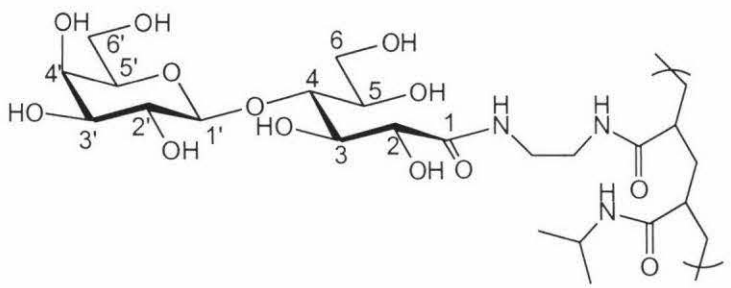

(60)

NMR δ (400Hz, D_2O) 4.53ppm (*br d*, 1'-H), 4.38ppm (*br s*, 2-H), 4.18(*br s*, 3-H), 3.95ppm—3.50ppm (*br m*, Lactone-H and NHC**H**), 3.45ppm (*br s* HNC**H**$_2$$CH_2$NH), 3.00ppm (*br s*, $HNCH_2$C**H**$_2$NH), 2.28—1.38ppm (*br*, Alkyl backbone); 1.10ppm (*br* s, (C**H**$_3$)$_2$).

4.3.5.2 Copolymer of N-acryloylethylene diamine ***(50)*** *and N-isopropylacrylamide*

N-Boc-acryloylethylene diamine **(49)** (300mg, 1.4mmol) was dissolved in 7ml of 2-methoxyethanol and *N*-isopropylacrylamide (159mg, 1.4mmol) was added to this solution. Nitrogen gas was bubbled through the solution for 30min to deoxygenate it,

then azo88 (6mg, 1.3 % w/w %) was added as the free radical initiator, and the solution stirred at 90°C under N_2 overnight. The solution was evaporated under reduced pressure, and the residue dissolved in 20ml of a 50:50 mixture of trifluoroacetic acid and DCM and stirred at room temperature for 30min. The solvent was removed under reduced pressure, and the residue dried *in vacuo.* The crude polyamine was dialyzed for two days against water with 8 changes per day. The solution was freeze-dried *in vacuo.*

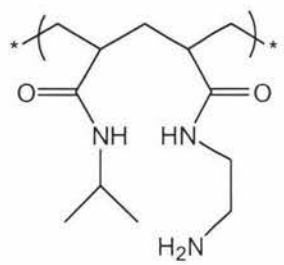

(59)

NMR δ (400Hz, D_2O) 3.86ppm(1H, *br* s, C**H**NH); 3.67ppm(2H, *br* s, NHC**H**$_2$); 3.09ppm(2H, *br* s, C**H**$_2$NH$_2$); 2.30—1.30ppm(6H, *br*, Alkyl backbone); 1.11ppm(6H, *br* s, (C**H**$_3$)$_2$).

NMR ^{13}C (500Hz, D_2O) 177.33ppm and 175.16ppm (C=O), 41.75ppm (NH**C**H), 38.79ppm (CONH**C**H$_2$), 37.04ppm (**C**H$_2$NH$_2$), 21.44ppm ((**C**H$_3$)$_2$)

FPLC: molecule weight range from 14,200 to 24,000g/mol

Schiff's reagent test: negative

*4.3.5.2.1 Lactosylated polyamine **(60)***

Polyamine **(59)** (200mg) that contained approximately 0.9mmol free amine groups was dissolved in 10 ml methanol with DIEA (150µl, 0.9mmol) and the lactone **(46)** (150mg, 0.44mmol). The solution was stirred at room temperature under a drying tube for 24hr. The solution was evaporated to dryness, and the residue was dialyzed against Milli-Q water for 24hr with periodic changes of water. Finally the solution was freeze-dried *in vacuo.*

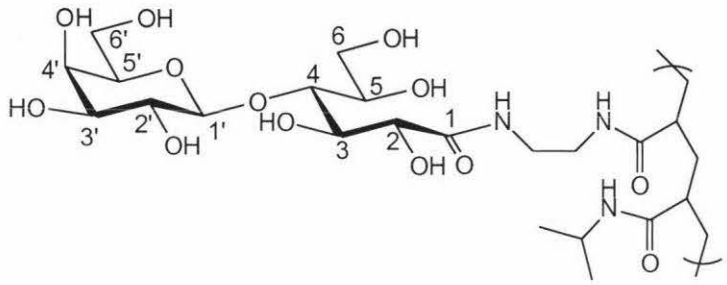

(60)

NMR δ (400Hz, D_2O) 4.53ppm (*br d J*=6.7Hz, 1'-H), 4.38ppm (*br s*, 2-H), 4.18(*br s*, 3-H), 3.95ppm—3.50ppm (*br m*, Lactone-H and NHC**H**), 3.45ppm(*br s* HNC**H**$_2$CH$_2$NH), 3.00ppm(*br s*, HNCH$_2$C**H**$_2$NH), 2.28—1.38ppm (*br*, Alkyl backbone); 1.10ppm (*br* s, (C**H**$_3$)$_2$).

FPLC: molecule weight range from 14,200 to 45,000g/mol

Schiff's reagent test: positive

4.3.5.2.2 Acryloyl-polyamide ***(61)***

Polyamine **(59)** (200mg, 0.88mmol) was dissolved in 20ml DMF and the solution was cooled in an ice bath. DIEA (306ul, 1.79mmol) was added. Acryloyl chloride (72ul, 0.88mmol) in 5ml DMF was added dropwise to the cold solution, and the solution warmed to room temperature and stirred under a drying tube for 24hr. The solvent was evaporated under reduced pressure. The residue was dialyzed against water for 2 days with 8 changes per day. The solution was freeze-dried. A solid white polymer was obtained.

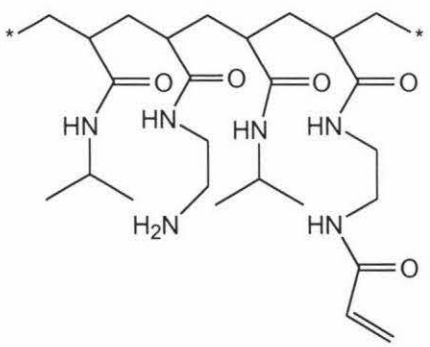

(61)

NMR δ (400Hz, D_2O) 6.22ppm (*br m*, CH_2=CH), 5.71ppm (*br d*, CH_2=C**H**), 3.86ppm(*br s*, C**H**NH); 3.38ppm(*br s*, NHCH_2); 3.09ppm(*br s*, CH_2NH); 2.30—1.30ppm(*br*, Alkyl backbone); 1.11ppm(*br s*, (CH_3)$_2$).

Acryloyl-polyamide **(61)** was dissolved in water (1.20ml), and N, N'-methylene-bisacrylamide (19mg, 0.13mmol) and ammonium peroxodisulphate (50mg, 0.22mmol) were added. The solution was deoxygenated by bubbling N_2 for 30min, followed by adding TEMED (300ul, 2.00mmol). The gel formed quickly.

4.3.5.2.3 Lactosylated Acryloyl polymer ***(62)***

Polyamine **(59)** (200mg, 0.88mmol) was dissolved in 20ml MeOH, DIEA (210ul, 1.20mmol) and lactone **(46)** (253mg) were added, the solution was stirred at room temperature under a drying tube for 24hrs. The solution was evaporated under reduced pressure to dryness, and the residue was dialyzed against water for 2 days with 8 changes per day. The solution was freeze-dried *in vacuo*. The residue was then dissolved in 25ml of water and the solution cooled in an ice-bath. DIEA (342ul, 2mmol), Acryloyl chloride (82µl, 1mmol) was added, the solution warmed to room temperature and stirred for 48hr. The solution was dialyzed for 2 days with 8 changes per day, and the solution then freeze-dired *in vacuo*.

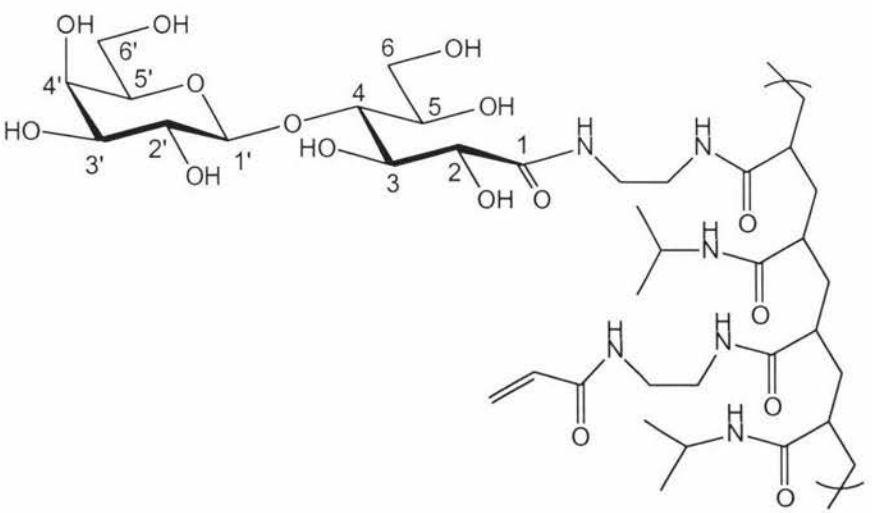

(62)

NMR δ (400Hz, D_2O) 6.22ppm (*br m*, CH_2=CH), 5.71ppm (*br d*, CH_2=C**H**), 4.53ppm (*br d J*=6.7Hz, 1'-H), 4.38ppm (*br s*, 2-H), 4.18(*br s*, 3-H), 3.95ppm—3.50ppm (*br m*, Lactone-H and NHC**H**), 3.45ppm-3.00ppm(*br s* HNCH_2CH_2NH), 2.28—1.38ppm (*br*, Alkyl backbone); 1.10ppm (*br* s, (CH_3)$_2$).

4.3.6 Preparation of Films and Sponges

4.3.6.1 Procedure for the preparation of Film from polyamine ***(59)***

Polyamine **(59)** (4mg) that contained free amino groups (0.0176mmol) was dissolved in 40μl water and acetic acid (8μl) was added. Glutaraldehyde-methanol solution (40μl, $8.8x10^{-3}$mmol) was added and the solution thoroughly mixed. The bottom of each of eight wells of a cell culture plate was coated with 10μl of the solution and then the plate was shaken gently for 24 hours. The thin films became red. The plate was placed into a methanol-water solution and $NaBH_4$ was added. After 12 hours the thin films became white. The films were washed as follows: 0.1M NaOH solution for 2 hours, distilled water ten changes for 24 hours, methanol. The films were then air-dried.

4.3.6.2 Procedure for the preparation of Film from lactosylated polyamine ***(60)***

Lactosylated polyamine **(60)** (2mg) that contained free amino groups (0.0025mmol) was dissolved in 40μl water and acetic acid (4μl) was added. Glutaraldehyde-methanol solution (40μl, $1.25x10^{-3}$mmol) was added and the solution thoroughly mixed. The bottom of each of eight wells of a cell culture plate was coated with 10μl of the solution and then the plate was shaken gently for 24 hours. The thin films became yellow. The plate was placed into a methanol-water solution and $NaBH_4$ was added. After 12 hours the thin films became white. The films were washed as follows: 0.1M NaOH solution for 2 hours, distilled water ten changes for 24 hours, methanol. The films were then air-dried.

*4.3.6.3 Procedure for the preparation of Sponges from lactosylated polyamine****(60)***

Partially lactosylated polyamine (50mg, 0.063mmol free amino groups), i.e. some pendant free amino groups, was dissolved in 1ml water and acetic acid (5μl) was

added. The solution was mixed and placed in the freezer until it froze solid, then it was transferred to the freeze drier. The residual round, white tablet was placed into a suitably sized vial. Acetonitrile (1ml) and glutaraldehyde (128µl, 2.5% CH_3CN solution) were added, and the vial was placed on a shaker and shaken gently overnight. The tablet (now yellow) was treated with $NaBH_4$. After the reduction the tablet became white again indicating that the reduction had finished. The tablet was washed with 0.1M NaOH solutions once for 2hours and then with Milli-Q system water for another 2 days with 8 changes per day and finally freeze-dried *in vacuo*.

References:

[1] Makarand R, "Tissue engineering implications in the treatment of organ and tissue defects", *Biogerontology* **2:** 117-125, 2001

[2] Whang K, Tsai DC, Nam EK, Aitken M, Sprague SM, Patel PK, Healy KE, "Ectopic bone formation via rhBMP-2 from porous bioabsorbable polymer scaffolds", *J Biomed Mater Res* **42:** 491-499, 1998

[3] Lanza RP, Jackson R, Sullivan A, Ringeling J, Mcgrath C, Kuhtreiber W, Chick WL, "Xenotransplantation of cells using biodegradable microcapsules", *Transplantation* **67:** 1105-1111, 1999

[4] Putnam AJ, Mooney DJ, "Tissue engineering using synthetic extracellular matrices", *Nat Med* **2:** 824-826, 1996

[5] Marler JJ, Upton J, Langer R, Vacanti JP, "Transplantation for cells in matrices for tissue regeneration", *Adv Drug Deliv Rev* **33:** 165-182, 1998

[6] Woerly S, Petrov P, Sykova E, Roitbak T, Simonova Z, Harvey AR, "Neural tissue formation within porous hydrogels implanted in brain and spinal cord lesions: ultrastructural immunohistochemical and diffusion studies", *Tissue Eng* **5:** 467-488, 1999

[7] Koechlin N, Pisam M, Poujeol P, Tauc M, Rambourg A, "Conversion of a rabbit proximal convoluted tubule (PCT) into a cell monolayer: ultrastructural study of cell differentiation and redifferentiation", *Eur J Cell Biol* **54:** 224-236, 1991

[8] Minuth WW, Aigner J, Kloth S, Steiner P, Tauc M, Jennings ML, "Culture of embryonic renal collecting duct epithelia in a gradient container", *Pediatr Nephrol* **163:** 140-147, 1997

[9] Butor C, Davoust J, "Apical to basolateral surface area ratio and polarity of MDBC cells grown on different supports", *J Exp Cell Res* **203:** 115-127, 1992

[10] Marchand BJ, Detrait E, Noiset O, Boxus T, Schneider YJ, Remacle C, "Biological evaluation of RGD peptidomimetics, designed for the covalent derivatization of cell culture substrata, as potential promotors of cellular adhesion", *Biomaterials* **20:** 1773-1782, 1999

[11] Thomson RC, Ishaug SL, Mikos AG, Langer R, "Polymers for biological systems", pp 717-724, In: R. A. Meyers (ed.), *Molecular biology and biotechnology*: A comprehensive desk reference. VCH, New York, 1995

[12] Bell CL, Peppas NA, "Water, solute and protein diffusion in physiologically responsive hydrogels of poly (methacrylic acid-g-ethylene glycol)", *Biomaterials* **17:** 1203-1218, 1996

[13] Jen AC, Wake MC, Mikos AG, "Review: Hydrogels for cell immobilization", *Biotech Bioeng* **50:** 357-364, 1996

[14] Hoffman AS, "Hydrogels for biomedical application", *Adv Drug Del Rev* **43:** 3-12, 2002

[15] Campoccia D, Doherty P, Radice M, Brun P, Abatangelo G, Williams DF, "Semisynthetic resorbable materials from hyaluronan esterification", *Biomaterials* **19:** 2101-2127, 1998

[16] Prestwich GD, Marecak DM, Marecak JF, Vercruysse KP, Ziebell MR, "Controlled chemical modification of hyaluronic acid", *J Cont Rel* **53:** 93-103, 1998

[17] Lee KY, Mooney DJ, "Hydrogels for tissue engineering", *Chem Revs* **101:** 1869-1879, 2001

[18] Hutmacher DW, "Scaffold design and fabrication technologies for engineering tissues. State of the art and future perspectives", *J Biomater Sci Polymer Ed* **12:** 107-124, 2001

[19] Leroux MA, Guilak F, Setton LA, "Comprehensive and shear properties of alginate gel : Effects of sodium ions and alginate concentration", *J Biomed Mater Res* 46-53, 1999

[20] Bromberg LE, Ron ES, "Temperature-responsive gels and thermogelling polymer matrices for protein and peptide delivery", *Adv Drug Deliv Rev* **31:** 197-21, 1998

[21] Huang S, Ingber DE, "The structural and mechanical complexity of cell-growth control", *Nature Cell Biol* **1:** E131-E138, 1999

[22] Lee KY, Rowley JA, Eiselt P, Moy EM, Bouhadir KH, Mooney DJ, "Controlling mechanical and swelling properties of alginate hydrogels independently by cross-linker type and cross-linking density", *Macromolecules* **33:** 4291-4294, 2000

[23] Jen AC, Wake MC, Mikos AG, "Review: Hydrogels for cell immobilization", *Biotech Bioeng* **50:** 357-364, 1996

[24] Giancotti FG, Ruoslahti E, "Transduction - integrin signalling", *Science* **285:** 1028-1032, 1999

[25] Cima L, Lopina S, Merrill E, "Ligand-modified PEO-based materials for cell transplantation", *Ann Biomed Eng* **22:** 184, 1994

[26] Smetana K, "Cell biology of hydrogels", *Biomaterials* **14:** 1046-1050, 1993

[27] Ratner B, "Hydrogel surface", pp. 85-94, In: N. A. Peppas (ed.), *Hydrogels in medicine and pharmacy*: Fundamentals. CRC Press, Boca Raton, FL, 1986

[28] Park K, Cooper SL, Robinson JR, "Bioadhesive hydrogels", pp151-176, In: N. A. Peppas (ed.), *Hydrogels in medicine and pharmacy*: Properties and applications. CRC Press, Roca Raton, FL, 1987

[29] Drumheller PD, Hubbell JA, "Surface immobilization of adhesion ligands for investigations of cell/substrates interactions", pp. 1583-1592, In: J. D. Bronzino (ed.), *Handbook of biomedical engineering*. CRC Press, Roca Baton, FL,1995

[30] Oxley HR, Corkhill PH, Fitton JH, Tighe BJ, "Macroporous hydrogels for biomedical applications: Methodology and morphology", *Biomaterials* **14:** 1064-1072, 1993

[31] Yannas IV, "Tissue regeneration templates based on collagen-glycosaminoglycan copolymers", *Bioploymers II* **122:** 219-244, 1995

[32] Koebe HG, Pahernik S, Eyer P, Schildberg FW, "Collagen gel immobilization: A useful cell culture technique for long-term metabolic studies on human hepatocytes", *Xenobiotica* **24:** 95-107, 1994

[33] Christensen L, Dionne K, Lysaught M, "Biomedical application of immobilized cells", pp 7-41, In: M.F.A. Goosen (ed.), *Fundamentals of animal cell encapsulation*. CRC Press, Boca Raton, FL, 1993

[34] Sefton MV, Stevenson WTK, "Microencapsulation of live animal cells using polyacrylate", *Adv Polym Sci* **107:** 143-197, 1993

[35] Chang TMS, "Hybrid artificial cells: Microencapsulation of living cells", *ASAIO J* **38:** 128-130, 1992

[36] http:\function of liver cell.htm

[37] Kobayashi A, Akaike T, Kobayashi K, Sumitomo H, "Enhanced adhesion and survival efficiency of liver cells in culture dishes coated with a lactose-carrying styrene copolymer", *Makromolek Chem – Rapid Commun.* **7:** 645-650, 1986

[38] Jared WA, Tarek H, Sangeeta NB, "Advances in bioartificial liver devices", *Hepatology* **34:** 447-55, 2001

[39] Smentana K, "Cell biology of hydrogels", *Biomaterials* **14:** 1046-50, 1993

[40] Weigel PH, Schmell E, Lee YC, Roseman S, "Specific adhesion of rat hepatocytes to beta-galactosides linked to polyacrylamide gels", *J Biol Chem* **253:** 330-333, 1978

[41] Langer R, Vacanti JP, "Tissue engineering", *Tissue Eng Sci* **260:** 920-926, 1993

[42] Sawada N, Tomomura A, Sattler CA, Sattler GL, Kleinman HK, Pitot HC, "Extracellular-matrix components influence DNA-sysntheis of rat hepatocytes in primary culture", *Exp Cell Res* **167:** 458-470, 1986

[43] Mooney D, Hansen L, Vacanti J, Langer R, Farmer S, Ingber D, "Switching from differentiation to growth in hepatocytes: control by extracellular matrix", *J Cell Physiol* **151:** 497-505, 1992

[44] Kobayashi A, Goto M, Kobayashi K, Akaike T, "Receptor-mediated regulation of differentiation and proliferation of hepatocytes by synthetic polymer model of asialoglycoprotein", *J Biomater Sci Polym Ed* **6:** 325-342, 1994

[45] Kobayashi K, Kobayashi A, Tobe S, Akaike T, "Carbohydrate-containing polystyrenes. In: Lee YC, Lee RT, editors. Neoglyco-conjugates: preparation and applications", *New York: Academic Press* 84-261, 1994

[46] Kobayashi K, Kobayashi A, Akaike T, "Culturing hepatocytes as on lactose-carrying polystyrene layer asialoglycoprotein receptor-mediated interactions", *Method Enzymol* **247:** 409-418, 1994

[47] Park IK, Yang J, Jeong HJ, Bom HS, Harada I, Akaie T, Kim S, Cho CS, "Galactosylated chitosan as a synthetic extracellular matrix for hepatocytes attachment", *Biomaterials* **24:** 2331-2337, 2003

[48] Muzzarelli R, Baldassare V, Conti F, Ferrara P, Biagini G, Gazzanelli G, Vasi V, "Biological activity of chitosan: ultrastructural study", *Biomaterials* **9:** 247-252, 1988

[49] Chung TW, Yang J, Akaike T, Kwang YC, Nah JW, Su K, Cho CS, "Preparation of alginate/galactosylated chitosan scaffold for hepatocyte attachment", *Biomaterials* **23:** 2827-2834, 2002

[50] Shoichet MS, Li RH, White ML, Winn SR, "Stability of hydrogels used in cell encapsulation; an in vitro comparison of alginate and agarose", *Biotech Bioeng* **502:** 81-374, 1996

[51] Heskins M, Guillet JE, "Solution properties of N-isopropylacrylamide" , *J. Macromol Sci, Chem* **A2:** 1441-1455, 1968

[52] Chen GH, Hoffman AS, "Graft-copolymers that exhibit temperature-induced phase–transitions over a wide-range of pH", *Nature* **373:** 49-52, 1995

[53] Vernon B, Gutowska A, Kim SW, Bae YH, "Thermally reversible polymer gels for biohybrid artificial pancreas", *Macromol Symp* **109:**155-167, 1996

[54] Taylor LD, Cerankowski LD, "Preparation of films exhibiting a balanced temperature-dependence to permeation by aqueous solution – study of lower consolute behaviour", *J Polym Sci Part A – Poly Chem* **13:** 2551-70, 1975

[55] Bae YH, Okano T, Kim SW, "On off thermocontrol of solute transport .1. Temperature-dependence of swelling of N-isopropylacrylamide networks modified with hydrophobic components in water", *Pharm Res* **8:** 531-537, 1991

[56] Hoffman AS, Afrassiabi A, Dong LC, "Thermally reversible hydrogel: II. Delivery and selective removal substances from aqueous solutions", *J Contr Rel* **4:** 213-222, 1986

[57] Yoshida R, Sakai K, Okano T, Sakurai Y, "Modulating the phase-transition temperature and themosensitivity in N-isopropylacrylamide copolymer gels", *J. Biomater Sci, Polym Ed* **6:** 585-598, 1994

[58] Stile RA, Burghardt WR, Healy KE, "Synthesis and characterization of injectable poly (N-isopropylacrylamide)-based hydrogels that support tissue formation in vitro", *Macromolecules* **32:** 7370-7379, 1999

[59] Morikawa N, Matsuda T, "Thermoresponsive artificial extracellular matrix: N-isopropylacrylamide-graft-copolymerized gelatin", *J Biomater Sci, Polym Ed* **13:** 167-83, 2002

[60] Matsuda T, "Molecular design of functional artificial extracellular matrix: thermoresponsive gelatin", *Jpn J Artif Organs* **28:** 242-5, 1999

[61] Ohya S, Nakayama Y, Matsuda T, "Material design for artificial extracellular matrix: cell entrapment in poly (N-isopropylacrylamide) (PNIPAM)-grafted gelatin hydrogel", *J Artif Organs* **4:** 308-14, 2001

[62] Ohya S, Kidoaki S, Matsuda T, "Poly(N-isopropylacrylamide) (PNIPAM)-grafted hydrogel surfaces: interrelationship between microscopic structure and mechanical property of surface regions and cell adhesiveness", *Biomaterials* **26:** 3105-3111, 2005

[63] Brazel CS, Peppas NA, "Pulsatile local delivery of thrombolytic and antithrombotic agents using poly(N-isopropylacrylamide-co-methacrylic acid) hydrogels", *J Contr Rel* **39:** 57-64, 1996

[64] Serres A, Baudys M, Kim SW, "Temperature and pH-sensitive polymers for human calcitonin delivery", *Pharm Res* **13:** 196-201, 1996

[65] Aoun SB, Bang GS, Koga T, Nonaka Y, Sotomura T, Taniguchi I, "Electrocatalytic oxidation of sugars on silver-UPD single crystal gold electrodes in alkaline solutions", *Electrochem Commun* **5:** 317-320, 2003

[66] Singh AK, Singh V, Rahmani S, Singh AK, Singh B, "Mechanism of Pd (II) and Hg (II) co-catalyzed oxidation of D-mannose and maltose by acidic solution of N-bromoacetamide", *J Molec Cat A: Chem* **197:** 91-100, 2003

[67] Moore S, Link KP, "Carbohydrate characterization", *J Biol Chem* **133:** 293-311, 1940

[68] Kobayashi K, Sumitomo H, Ina Y, "Synthesis and functions of polystyrene derivatives having pendant oligosaccharides", *Polymer J* **17:** 567-575, 1985

[69]] Solomons TW, Organic chemistry, John Wiley & Sons, Inc., Canada, Chapter 18.8 E: 788-789, 1992

[70] Glümer A, Skeries BD, Buchholz K, "Synthesis and copolymerization of unsaturated glucono-δ-lactone derivatives", *Macromol Chem Phys* **205:** 73-82, 2004

[71] Motherwell WB, Atkinson CE, Aliev AE, Wong SY, Warrington BH, "A simple protocol for the modular assembly of "Millipede" artificial enzymes", *Angew Chem Int Ed* **43:** 1225-1225, 2004

Appendix: Initial Cell Trial Results

Cell trials were performed by on-campus collaborators (Ms L Green and Associate Professor K Pedley, Institute of Food Nutrition and Human Health). The trials involved growing cells for 1 day on control (plastic) surfaces, or on thin polymer films spread over the control surface, and examination of cell numbers and morphology by bright field (visible light) and fluorescence microscopy.

A.1 HeLa cell trials (bright field)

Initial cell trials were with the HeLa cells, which are robust human epithelial cells. This cell line does not closely model hepatocytes, but provides an indication of the overall cyto-compatibility of the substratum. Acceptable surfaces support cell proliferation to form a confluent layer of flattened cells (Figure A.1).

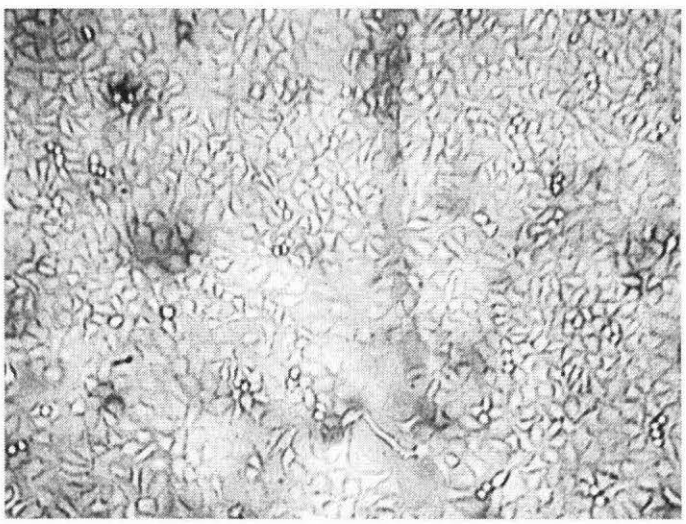

Figure A.1. Confluent layer of HeLa cells growing on a control (plastic) surface

HeLas were found to grow very poorly on the "bare" polyamine **(59)**. After 24hrs incubation, very few viable cells were visible under bright field microscopy (Figure A.2). In contrast, HeLas grew readily on the lactosylated polyamine **(60)** (Figure A.3).

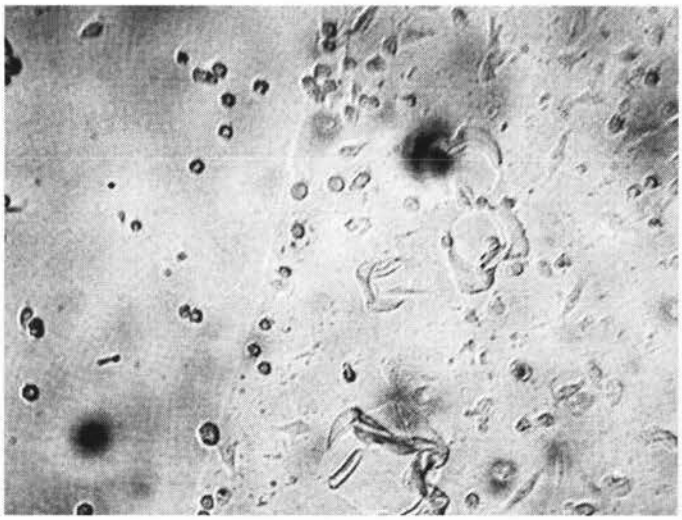

Figure A.2. HeLa cell trial on polyamine thin film (polymer film on the right, control surface on the left)

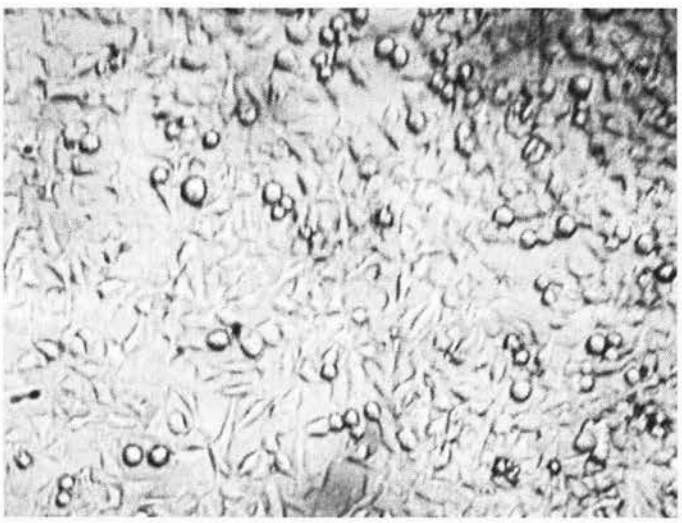

Figure A.3. HeLa cells growing on lactosylated polymer **(60)** thin film

6.2 HeLa cell trials (fluorescence)

BCECF is a carboxylated derivative of fluorescein. The methyl ester form of BCECF is readily absorbed into cells, where the action of esterases causes hydrolysis to the free acid form, which cannot permeate the cell membrane. Fluorescence therefore accumulates only in viable cells that have sound membranes and active esterases present, and so BCECF has found widespread use as an indicator of cell viability.

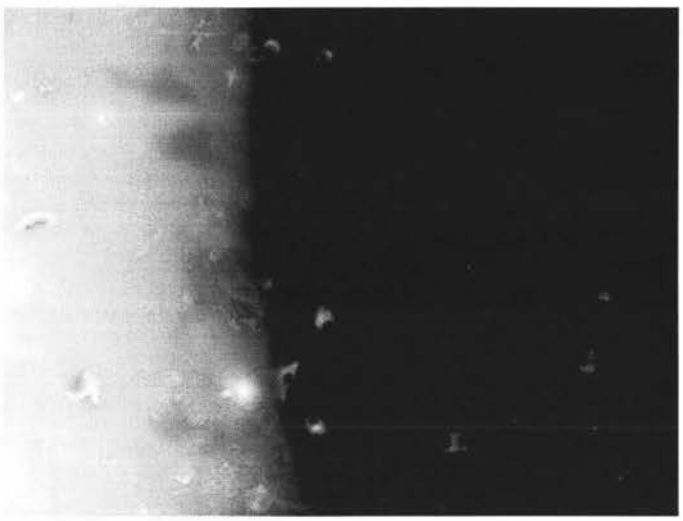

Figure A.4. Fluorescence microscopy of Hela cells on polyamine film **(59)** (polymer film on left, control surface on right)

Polyamine **(59)** was strongly fluorescent following treatment with BCECF (Figure A.4), presumably through salt or amide formation between the free amino groups of the polymer and the acid groups of the dye. This made it difficult to detect cells on the polymer surface. The lactosylated polymer **(60)** presents fewer amino groups and hence produced much weaker background fluorescence (Figure A.5.). Many viable cells are visible on the polymer surface, in agreement with the observations from bright-field microscopy.

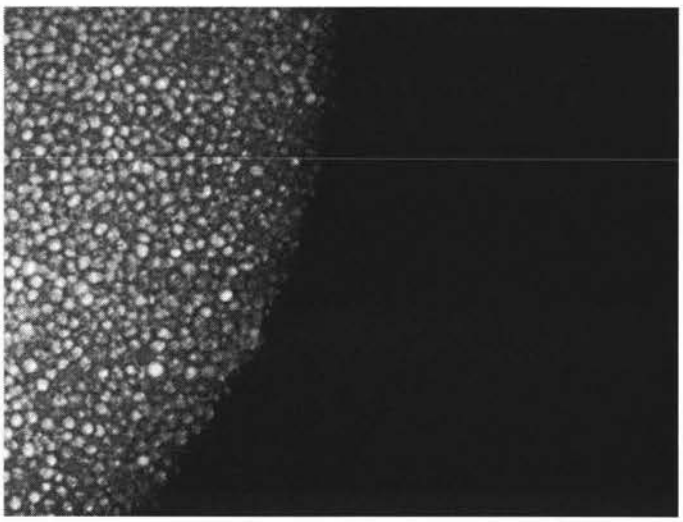

Figure A.5. Fluorescence microscopy of Helas on lactosylated polymer **(60)** thin film (polymer on left, control surface on right)

Thus it is clear that HeLa cells did not accept the polyamine **(59)** thin film as a substratum, but with the lactosylated polymer **(60)** the polymer surface was preferred over the control surface.

6.3 HepG2 cells trials

The lactosylated polymer (60) was further trialled with HepG2 cells, which are cells from human liver tumours and therefore provide a closer approximation to hepatocyte behaviour. These cells prefer to form ball-like colonies.

It was found that HepG2 cells grew readily on the lactosylated polymer **(60)**. Furthermore, the clumps broke up and the cells spread out in a monolayer over the surface (Figures A.6 and A.7), indicating that the cells prefer contact with the substratum over cell-cell contacts.

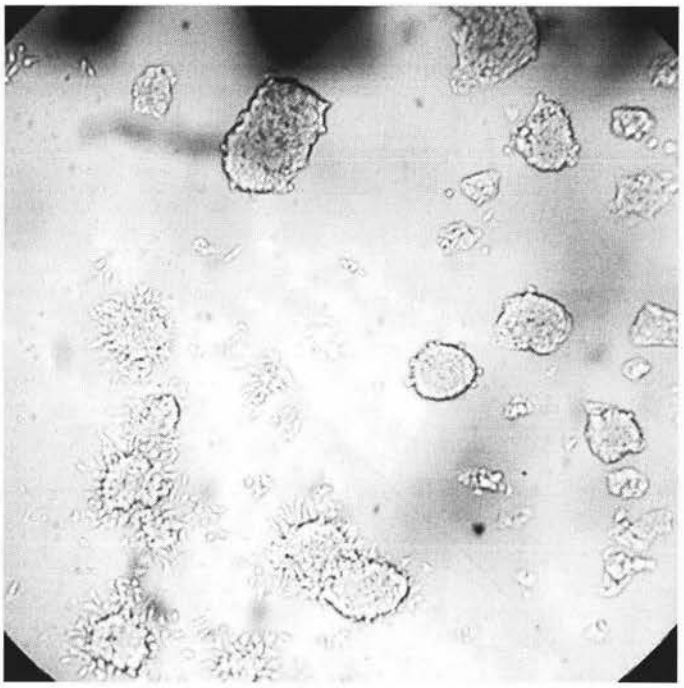

Figure A.6. Bright-field microscopy of HepG2 cells on lactosylated polymer **(60)** thin film (polymer bottom left, control surface top right)

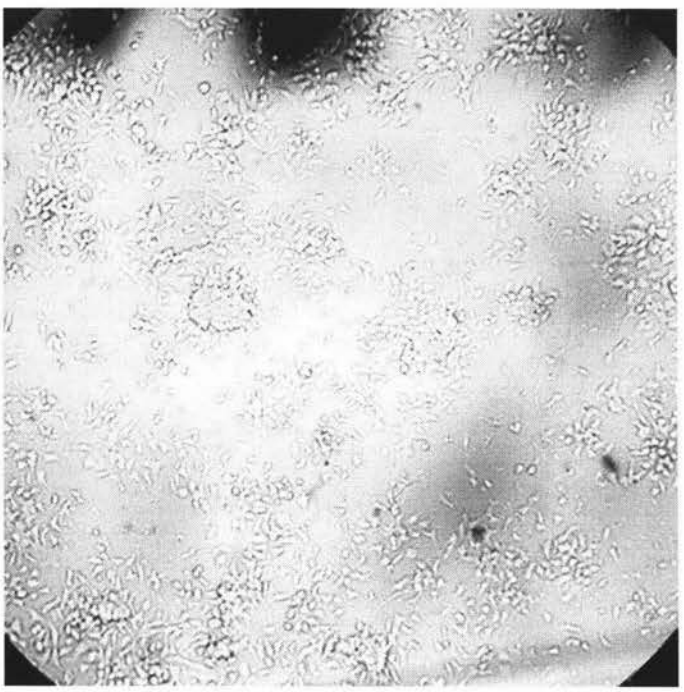

Figure A.7. Bright-field microscopy of HepG2 cells on lactosylated polymer **(60)** thin film